Received: 23 March 2023 | Accepted: 21 June 2023

DOI: 10.1002/ajb2.16218

RESEARCH ARTICLE

American Journal of Botany

Genome-material costs and functional trade-offs in the autopolyploid *Solidago gigantea* (giant goldenrod) series

Angela M. Walczyk[1,2] | **Erika I. Hersch-Green**[1]

[1]Department of Biological Sciences, Michigan Technological University, 1400 Townsend Drive, Houghton, MI 49931, USA

[2]Biology Department, Gustavus Adolphus College, 800 West College Avenue, St. Peter, MN 56082, USA

Correspondence

Erika I. Hersch-Green, Department of Biological Sciences, Michigan Technological University, 1400 Townsend Drive, Houghton, MI 49931 USA.
Email: eherschg@mtu.edu

Abstract

Premise: Increased genome-material costs of N and P atoms inherent to organisms with larger genomes have been proposed to limit growth under nutrient scarcities and to promote growth under nutrient enrichments. Such responsiveness may reflect a nutrient-dependent diploid versus polyploid advantage that could have vast ecological and evolutionary implications, but direct evidence that material costs increase with ploidy level and/or influence cytotype-dependent growth, metabolic, and/or resource-use trade-offs is limited.

Methods: We grew diploid, autotetraploid, and autohexaploid *Solidago gigantea* plants with one of four ambient or enriched N:P ratios and measured traits related to material costs, primary and secondary metabolism, and resource-use.

Results: Relative to diploids, polyploids invested more N and P into cells, and tetraploids grew more with N enrichments, suggesting that material costs increase with ploidy level. Polyploids also generally exhibited strategies that could minimize material-cost constraints over both long (reduced monoploid genome size) and short (more extreme transcriptome downsizing, reduced photosynthesis rates and terpene concentrations, enhanced N-use efficiencies) evolutionary time periods. Furthermore, polyploids had lower transpiration rates but higher water-use efficiencies than diploids, both of which were more pronounced under nutrient-limiting conditions.

Conclusions: N and P material costs increase with ploidy level, but material-cost constraints might be lessened by resource allocation/investment mechanisms that can also alter ecological dynamics and selection. Our results enhance mechanistic understanding of how global increases in nutrients might provide a release from material-cost constraints in polyploids that could impact ploidy (or genome-size)-specific performances, cytogeographic patterning, and multispecies community structuring.

KEYWORDS

genome size, material costs, nitrogen, nutrient-use, phosphorus, photosynthesis, polyploidy, transcriptome size

Polyploidization, or whole-genome duplication (WGD), results in three or more sets of homologous chromosomes per cell and can occur along a continuum of parental divergence from within a single species lineage (autopolyploidy) to concurrently with hybridization (allopolyploidy; Stebbins, 1950). In angiosperms, both WGD processes commonly occur (Wood et al., 2009; Jiao et al., 2011; Barker et al., 2016; Parisod and Broennimann, 2016), inducing morphological, phenological, and/or physiological trait changes that are associated with structural, functional, and/or epigenetic modifications of genomes (Song et al., 1995; Ramsey and Schemske, 2002; Osborn et al., 2003; Chen, 2007; Wendel, 2015; Barker et al., 2016). As a result, the ecological and evolutionary consequences of WGD are plentiful and varied, sometimes contributing to enhanced tolerances to environmental stressors, novel gene expression profiles, and accelerated rates of adaptation and diversification, and in other cases contributing to decreased tolerances to environmental stressors, increased accumulations of deleterious mutations, masking of beneficial recessive mutations, and reduced rates of adaptation and diversification (Stebbins, 1971; Otto and Whitton, 2000; Soltis and Soltis, 2000; Comai, 2005; Mayrose et al., 2015; Van de

Peer et al., 2017; Levin, 2019). Such varied responses to WGD preclude many generalities (e.g., Gaynor et al., 2020) and likely arise, in part, because different genome processes contribute to polyploid formation (e.g., allo- versus autopolyploidy, which differentially affects genome, transcriptome, and phenotype traits) and because organisms experience different environmental contexts, both of which influence evolutionary dynamics such as genetic drift and selection. To capture generalities of the ecological and evolutionary significance of duplicating genomes per se, we need to examine how polyploids respond to environmental conditions that similarly influence both auto- and allopolyploids.

One environmental condition that should similarly influence auto- and allopolyploids is soil nitrogen (N) and phosphorus (P) availability. Genome size (GS) scales positively with ploidy level for both auto- and allopolyploids (Blommaert, 2020), and N and P limitations are predicted to be a disadvantage for organisms with larger GS because they have greater material costs for N and P in their genome (Lewis, 1985; Leitch and Bennett, 2004; Cavalier-Smith, 2005). Increased material costs of organisms with larger GS are thought to arise because (1) DNA requires N and P atoms for synthesis (e.g., nucleic acids plus the sugar–phosphate backbone are approximately 12.5% N and 3.4% P; Elser et al., 2011), and (2) organisms with larger GS have larger cells (Beaulieu et al., 2008; Mueller, 2015; Roddy et al., 2020) that require more P to synthesize the associated longer phospholipid bilayer cell membranes. Furthermore, to maintain functional gene balance and genetic network stability after WGD, polyploids might also need to synthesize more proteins and rRNA, which would represent additional polyploid N and P cellular sinks (Birchler and Veitia, 2010; Hessen et al., 2013; Anneberg and Segraves, 2020). In contrast, nutrient enrichments may release polyploids from genome-material-cost constraints and enhance genetic and phenotypic advantages associated with polyploidy (Faizullah et al., 2021), such as being larger and more competitive (Thébault et al., 2011; Yang et al., 2021). In support of these predictions, studies have found that polyploidy and GS are positively correlated with cellular N and/or P content (Jeyasingh and Weider, 2007; Kang et al., 2015) and that environmental scarcities in N and/or P often favor the growth and fitness of diploids or organisms with smaller genomes, whereas N and/or P enrichments often have opposite effects, favoring the growth and fitness of organisms with larger genomes (Hessen et al., 2013; Neiman et al., 2013; Šmarda et al., 2013; Guignard et al., 2016; Bales and Hersch-Green, 2019; Walczyk and Hersch-Green, 2019; Anneberg and Segraves, 2020; Peng et al., 2022). However, a lack of ploidy-level- and GS-dependent growth responses to nutrient amendments has also been observed (Sánchez Vilas and Pannell, 2017; Walczyk and Hersch-Green, 2022), suggesting additional factors inherent to specific organisms and their environments likely contribute to realized material costs, selective constraints, and responses to nutrient availabilities.

Differences in RNA production, which represents the largest nucleic acid fraction in the cell and is a major N and P sink (Raven, 2013), may influence realized material costs and associated selective constraints. While the genome constitutes a static nutrient requirement for cells, the size of the transcriptome is plastic and can vary dependent upon nutrient supplies (Jeyasingh and Weider, 2007; Hessen et al., 2010; Raven, 2013) and ploidy level (Osborn et al., 2003; Grover et al., 2012; Dodsworth et al., 2015; Wendel et al., 2016). In fact, transcriptome downsizing, in which transcriptomes of polyploids are smaller than the sum of the progenitor transcriptomes, has been documented in polyploids and found to be more extreme than genome downsizing (Coate and Doyle, 2010; Doyle and Coate, 2019). Furthermore, nutrient limitations have been shown to selectively alter the elemental composition of DNA and RNA molecules toward reduced nutrient demands (i.e., more A-T/U than G-C pairings; Wagner, 2007; Bragg and Wagner, 2009; Acquisti et al., 2009a, 2009b) and organisms exposed to N and P (NP) limitations contain lower proportions of NP-rich amino acids and proteins (reviewed by Elser et al., 2011; Kelly, 2018; Majda et al., 2021). Therefore, polyploids might minimize their overall material costs by reducing their total RNA production and/or by preferentially downregulating N and/or P costly mRNA transcripts (Coate and Doyle, 2010; Faizullah et al., 2021; Wang et al., 2021a), and such transcriptome downsizing and selective transcript expression may be most pronounced under nutrient scarcities. This response would increase polyploid tolerance to nutrient-poor conditions, while also offering them flexibility to allocate nutrients to different functions when nutrients are more plentiful, thereby enhancing the genetic and phenotypic advantages to being polyploid.

Differences in N and P investments into primary and secondary metabolic pathways, such as photosynthesis and associated growth and/or defense processes, could also affect realized material costs. For instance, proteins, pigments, ATP, and/or electron transport molecules used directly in photosynthesis and growth (e.g., RuBisCo accounts for 20–30% of total leaf N in C_3 plants; Evans, 1989; Hessen et al., 2010; Hohmann-Marriott and Blankenship, 2011) and indirectly as precursors for defensive compound production (Yactayo-Chang et al., 2020; Ninkuu et al., 2021) also represent significant N and/or P sinks. Therefore, these macromolecules might compete with nucleic acids for N and/or P—potentially leading to resource allocation trade-offs between nutrient investments into nucleic acids versus investments into photosynthetic, growth, and/or defense (Kelly, 2018; Faizullah et al., 2021). While polyploidy and GS variation can influence plant growth rates (Wyngaard et al., 2005; Beaulieu et al., 2008; Corneillie et al., 2018), photosynthetic capacities (Warner and Edwards, 1993; Vyas et al., 2007; Cao et al., 2018; Simonin and Roddy, 2018; Roddy et al., 2020; Chen et al., 2021; Wang et al., 2021b; Walczyk and Hersch-Green, 2022) and defensive compound production (Gaynor et al., 2020), patterns are nuanced and differ among species, time since WGD events occurred, and whether increases in

GS arose via WGD, hybridization, and/or other processes—all of which may be further affected by environmental factors such as nutrient availabilities. Interestingly, in comparison to diploids, polyploids have been found to grow more in NP-enriched conditions and produce fewer seeds in N-limiting conditions (Šmarda et al., 2013; Guignard et al., 2016; Bales and Hersch-Green, 2019; Walczyk and Hersch-Green, 2019; Anneberg and Segraves, 2020), suggesting that greater relative NP investments into nucleic acids versus other functions in polyploids might be most apparent when nutrients are limiting and that nutrient enrichment releases selective constraints and favors polyploids.

Differences in organismal traits that influence access to and/or requirements of nutrients could also affect realized material costs, NP investment trade-offs, and/or patterns of selection. For instance, organisms with life-history traits rendering them less limited by nutrient availabilities, such as geophytes, legumes, or perennial plants, have been found to have larger genomes (Choi et al., 2004; Enke et al., 2011; Veselý et al., 2013; Hloušková et al., 2019; Qiu et al., 2019), potentially implying less dependency on variable environmental nutrient supplies for genome-material costs. Furthermore, organismal differences in stomatal attributes that vary with ploidy level can affect photosynthesis and transpiration rates and thus requirements for nutrients and water (Faizullah et al., 2021). For example, plants with fewer and larger stomata per unit leaf area (which is characteristic of larger GS plants; Knight and Beaulieu, 2008) have been shown to have lower stomatal conductance, transpiration, and photosynthetic rates (Lawson and Blatt, 2014; Roddy et al., 2020; Théroux-Rancourt et al., 2021; but see Knight and Beaulieu, 2008). Lastly, organisms with higher nutrient-use efficiencies (i.e., are better able to access and utilize nutrients) are expected to be more tolerant of nutrient scarcities, and faster growing plants (such as diploids with smaller GS) have been shown to be more efficient at using N for photosynthesis (Robinson et al., 2001; Hikosaka, 2004). While it is not known whether polyploidy directly influences nutrient-use efficiencies (but see Bales and Hersch-Green, 2019), plants that are less efficient at using N for photosynthesis (i.e., require more N to fix CO_2) experience stronger selection pressures to reduce N elemental costs in transcripts compared to plants that do not require as much N to fix CO_2 (Kelly, 2018; Majda et al., 2021).

To increase our understanding of the ecological and evolutionary consequences of WGD and GS variation, we examined diploid, autotetraploid, and autohexaploid cytotypes of *Solidago gigantea* (giant goldenrod, Asteraceae) under varying N and P availabilities. Studying an autopolyploid series allowed us to more precisely isolate responses due to larger genomes rather than increased heterozygosity, which is also associated with allopolyploidy. Specifically, we addressed six interrelated hypotheses. (Hypothesis [H] 1) Genome downsizing has occurred in this autopolyploid series, potentially indicating selection to reduce material costs. (H2) Plants with larger genomes have greater N and P material costs and are more growth-limited by NP scarcities. (H3) Plants regulate their total RNA production dependent upon ploidy level and nutrient availability. Specifically, we predicted that smaller GS cytotypes would have relatively larger transcriptomes (relative to their genome sizes) than larger GS cytotypes would, but that discrepancies would lessen under nutrient enrichments as material-cost constraints relax on polyploids. (H4) Rates of photosynthesis and concentrations of chemical defense compounds vary among cytotypes dependent upon nutrient availabilities. Specifically, we predicted that because photosynthesis and terpenes (a defensive compound within *Solidago*; Bohlmann et al., 1998; Bustamante et al., 2020; Ninkuu et al., 2021) both directly or indirectly (from precursor production) require N and P, that photosynthetic rates and terpene concentrations would be (1) higher under nutrient enrichments, (2) lower for larger GS cytotypes (due to material cost and photosynthesis/defense trade-offs), and (3) more similar among cytotypes under nutrient enrichments because larger GS cytotypes should be less constrained by material costs. (H5) Because stomatal density is negatively correlated with ploidy level in *S. gigantea* (Walczyk and Hersch-Green, 2022; Walczyk, 2022), larger GS cytotypes have lower transpiration rates and combined with how GS and nutrient availability influences photosynthesis (see H4) will also be more water-use efficient (able to assimilate more carbon from photosynthesis than water lost from transpiration) than smaller GS cytotypes, especially under nutrient-limiting conditions. (H6) Larger GS cytotypes are more nutrient-use efficient under nutrient limiting conditions, thereby minimizing increased material-cost constraints.

MATERIALS AND METHODS

Plant material

Solidago gigantea Aiton (giant goldenrod, Asteraceae) is a perennial aster native to North America where it exhibits cytotype variation due to WGD within the species (autopolyploidy; Beck and Semple, personal communication). Cytotypes are strongly spatially segregated and rarely co-occur with diploids ($2n = 2x = 18$) growing along the Atlantic Coast, tetraploids ($2n = 4x = 36$) growing within the Great Lakes region, and hexaploids ($2n = 6x = 54$) growing within the Great Plains region (Schlaepfer et al., 2008; Hull-Sanders et al., 2009). Tetraploids are the most widespread geographically and climatically given their status as a noxious invasive species in Europe and Asia (Schlaepfer et al., 2008; Hull-Sanders et al., 2009). During the summers of 2017 and 2019, we collected seeds and leaves from 21 populations covering the range of *S. gigantea* and determined the ploidy level of 528 plants (Verloove et al., 2017; Appendix S1).

Experimental design

After confirming that intrapopulation ploidy-level variation was mainly absent in our sampling (Walczyk and

Hersch-Green, 2022), we planted 240 seeds from different half-sibling maternal lines from populations of diploid ($N = 3$), tetraploid ($N = 4$), or hexaploid ($N = 3$) cytotypes in 2-L round pots containing a 50:50 mixture of vermiculite to Sun Grow Mix 1 potting soil (Sun Grow Horticulture, Agawam, MA, USA) in a greenhouse at Michigan Technological University (Department of Biological Sciences, Houghton, MI, USA) with lights on a 16:8 h light:dark cycle at ~23°C. At 3 weeks growth, plants were randomly assigned to one of four soil N:P treatments (ambient:ambient, ambient:enriched, enriched:ambient, enriched:enriched, $N = 20$ plants per cytotype per treatment). We chose to compare ambient to enriched nutrient levels to test the degree to which predicted increases in N and P from anthropogenic activity preferentially favor one cytotype over others. The vermiculite–potting soil mix contained 55 ppm N (μg N g^{-1}) and 12.5 ppm P (μg P g^{-1}), and we designated this mixture as the ambient N and P treatments because the nutrients were similar to N and P levels reported in global grassland ecosystems (e.g., dissolved available N range reported as 15–65 ppm, Christou et al. 2005; dissolved available P range reported as 1.2–29.0 ppm, Graça et al. 2022). For the enriched treatments, we added nutrients to pots to achieve enriched treatments with 110 ppm N (μg N g^{-1}) or 25 ppm P (μg P g^{-1}). Treatments were administered as 20 mL solutions of ammonium nitrate (enriched N), potassium monophosphate (enriched P), and/or water (ambient N and ambient P) on weeks 3 and 4 of growth; all pots received 40 mL total of these solutions plus 20 mL of a potassium sulfate (100 ppm; μg K g^{-1}) and micronutrients (Fertilome chelated liquid iron and other micronutrients; Voluntary Purchasing Groups, Bonham, TX, USA) solution. Pots were rotated and watered weekly, and the experiment concluded after 15 weeks of growth. Two diploids died during the experiment and were excluded from analyses.

Measured traits

We measured traits associated with material costs, primary metabolic processes, defense, and nutrient-use to test for evidence of material cost-mediated responses.

Genome size

After 5 weeks of plant growth, we collected one leaf from each plant to estimate holoploid GS ([2C-DNA content]; total amount of DNA in replicated chromosome sets) using flow cytometry (Appendix S1) and monoploid GS (1Cx-DNA content; total amount of DNA in unreplicated chromosome sets; Greilhuber et al., 2005) by dividing holoploid GS by plant ploidy level (2, 4, or 6 for diploids, tetraploids, or hexaploids, respectively); the precise GS of 18 plants could not be determined due to low-quality data and were excluded from GS analyses, although we were able to determine the ploidy level of 10 of these plants and included them in analyses that incorporated ploidy level.

RNA

After 10 weeks of plant growth, we harvested the youngest fully mature leaf of 114 plants (38 plants per cytotype divided evenly among ambient and enriched NP treatments) and immediately weighed, flash-froze, and transferred them to a −80°C freezer. Total RNA was then extracted from leaves using RNeasy Plant Extraction kits (QIAGEN, Hilden, Germany) following manufacturer's instructions and quantified with a Qubit Fluorometer (Thermo Fisher Scientific, Waltham, MA, USA). To verify repeatability, we also extracted duplicate RNA from the same leaf tissue of 20 plants. Although we did not detect repeatability issues, 15 RNA extractions failed or had unusually low yields ($N = 6$ for 2*x*, 5 for 4*x*, 4 for 6*x*) and were excluded from subsequent analyses.

Cell density

From a subset of leaves used to estimate foliar nutrients (see below), we estimated cell density following the methods of Brown and Rickless (1949). Briefly, a 2-cm-diameter leaf punch was taken from 52 plants ($N = 22$ for 2*x*, 27 for 4*x*, 27 for 6*x*), weighed, digested in chromic acid, and the number of cells in a 10-μL aliquot was counted on a hemocytometer to estimate cell density per milligram leaf tissue.

Foliar nutrients

After 11 weeks of plant growth, we harvested, ground, and homogenized three leaves (collected from the middle stem of plants) from two individuals of the same maternal line for each cytotype by nutrient combination. From this tissue, material foliar [N] was determined for 116 samples ($N = 37$ for 2x, 39 for 4x, 40 for 6x) with an elemental analyzer (Costech Analytical Technologies, Valencia, CA, USA) at the University of Minnesota, and foliar [P] was determined from 65 random samples (N = 19 for 2x, 29 for 4x, 17 for 6x) on a Thermo 6500 Duo Inductively Coupled Plasma Spectrometer (Thermo Fisher Scientific) at Brookside Laboratories (New Bremen, OH, USA) following acid digestion (Masson et al., 2010).

Photosynthesis, evapotranspiration, and water-use efficiency

We used a portable infrared CO_2 analyzer system (LI-6800; LI-COR Inc., Lincoln, NE, USA) equipped with a CO_2 mixer and $1 \times 3\ cm^2$ chamber/red-blue LED light source to measure maximum carbon assimilation rates between CO_2 fixation and photorespiration (A_{max}, μmol CO_2 m^{-2} s^{-1}) and evapotranspiration rates (E, mmol H_2O m^{-2} s^{-1}). From these values, we calculated instantaneous water-use efficiency (WUE_i) as A_{max}/E (μmol CO_2 mmol H_2O^{-1}). The youngest set of fully mature leaves was used for all measurements over 3 days during the 12th week of growth between the hours of 09:00 to 16:00. Inside the chamber, we set CO_2 concentration to 400 ppm, relative humidity to 65%, flow rate to 500 μmol m^{-2} s^{-1}, light to 1000 μmol m^{-2} s^{-1}, and temperature to 23°C. Measurements were taken once photosynthetic rate stabilized, and infrared gas analyzers (IRGA) were matched after every 10 measurements.

Foliar terpenes

After 11 weeks of plant growth, we harvested the youngest two fully mature leaves of 65 plants ($N = 23$ for $2x$, 22 for $4x$, 20 for $6x$) from ambient N and P and enriched N and P treatments and immediately weighed, flash-froze, and transferred them to a −80°C freezer. Terpenes were extracted following the methods of Hull-Sanders et al. (2009), and concentrations were quantified using a Trace 1310 Gas Chromatograph coupled with an ITQ 1100 Ion Trap MS (Thermo Fisher Scientific) using an Rtx-5MS (30 m × 0.25 mm; DF = 0.25 um) Low-Bleed GC/MS column (fused silica; Restek, Bellefonte, PA, USA) at Michigan Technological University (Houghton, MI, USA). Terpene peaks were grouped by retention times, identified using the machine's NIST2000 software database and the Mass Spectrometry Data Center (Chemdata.nist.gov), and cross-checked against other studies of terpenes involving *Solidago* species (Johnson et al., 2007; Hull-Sanders et al., 2009; Dobjanschi et al., 2019). We measured terpene concentrations for mono-, di-, and sesquiterpenes by averaging concentration values for each terpene across three technical replications and then summing the concentration values for each terpene group within each individual sample; seven samples ($N = 1$ for $2x$, 2 for $4x$, 4 for $6x$) yielded low quality data and were removed from analysis.

Biomass

Because many trait measurements required removal of leaves, we removed the same number of leaves that were ontogenically comparable for all plants over the course of the experiment to help account for these losses in our biomass calculations. At 15 weeks growth, plants were divided into above- and belowground parts, dried at 60°C for 48 h (aboveground) or 72 h (belowground) and weighed.

Statistical analyses

We used analysis of variance (ANOVA) models with different combinations of cytotype ($2x$ = diploid; $4x$ = tetraploid; $6x$ = hexaploid), soil-N:P treatment (ambient-N:P = ambient-N, ambient-P; enriched-N:P = enriched-N, enriched-P), N treatment (ambient-N; enriched-N), P treatment (ambient-P; enriched-P), and population of origin (nested within cytotype) specified as fixed-effect independent variables. Model assumptions of normality and homoscedasticity were examined, and data transformations to meet model assumptions were made as needed and noted below. For comparing significant differences among means, (1) when a single factor or interaction among nutrients was found to be significant, we used post-hoc Tukey's honestly significant difference (HSD) test, and (2) when a significant interaction among factors involving cytotypes was found, we used controlled contrast tests to compare means as detailed below. JMP Pro version 16.0 (SAS Institute, Cary, NC, USA) was used for all analyses.

Genome size

Separate ANOVA models were used to test whether holoploid (2C-DNA content) and/or monoploid GS (1Cx-DNA content) significantly differed among cytotypes and/or a plant's population of origin ($N = 222$).

Material costs and biomass accumulation

We directly examined material costs as N or P investments per milligram of tissue and per cell ([N] or [P] per milligram of tissue divided by cell density per milligram of tissue) with four separate ANOVA models using cytotypes, N treatment, P treatment, their interactions, and a plant's population of origin as factors ($N = 116$ for [N], $N = 65$ for [P]). Next, we used separate ANOVA models to test whether above- or belowground biomasses significantly differed among cytotypes, N treatments, P treatments, their interactions, and/or a plant's population of origin ($N = 236$). Lastly, because plants that are more limited by nutrients are thought to respond more strongly to nutrient additions (Boyer, 1982; Anneberg and Segraves, 2020), we also indirectly assessed material costs by examining growth responses to nutrient enrichments using the general formula:

$$\text{Growth response to nutrient enrichment} = \frac{\begin{array}{l}(\text{Combined biomass in enriched treatment} \\ -\ \text{Combined biomass in ambient treatment})\end{array}}{\begin{array}{l}\text{Average combined biomass across ambient} \\ \text{and enriched treatments}\end{array}}.$$

Growth responses to nutrient enrichments were calculated separately for N and P and for above- and belowground biomass responses ($N = 10$ per cytotype per nutrient for both above- and belowground) and combined biomasses were determined by taking the average for two individuals grown from the same maternal line within a given treatment. Four separate ANOVA models were used to assess whether cytotypes significantly differed in above- and/or belowground N and/or P growth responses.

Transcriptome size

We calculated transcriptome size as total RNA concentration ([RNA]) per cell (pg/cell) from the extracted RNA per milligram of tissue and cytotype cell density averages per milligram of tissue and we calculated relative transcriptome size ([RNA]/[2C-DNA content]) by dividing this value by cell 2C-DNA content from flow cytometry. Next, we examined whether either transcriptome metric significantly differed among cytotypes, soil-N:P treatments, their interaction, and/or a plant's population of origin with separate ANOVA models ($N = 99$; 32 for 2*x*, 33 for 4*x*, 34 for 6*x*).

Primary metabolic properties

We examined whether A_{max}, *E*, and/or WUE_i significantly differed among cytotypes, N treatments, P treatments, their interaction, and/or a plant's population of origin using separate ANOVA models ($N = 232$).

Nutrient-use efficiency

We measured nutrient-use efficiencies by first calculating metrics that describe plant effectiveness at incorporating soil nutrients into biomass (N-use efficiency [NUE] and P-use efficiency [PUE]) as aboveground dry biomass (g)/[N or P] (mg) in the soil (Moll et al., 1982; Islam et al., 2021). Next, we calculated metrics that describe how well plants use nutrients to fix CO_2 as photosynthetic nitrogen (P_{NUE})- and photosynthetic phosphorus (P_{PUE})-use efficiency by dividing the average A_{max} rates of the plants combined for N or P content by [N or P] (mg mg^{-1}) of leaf tissue. ANOVA models were then used to assess whether cytotypes, N treatments, P treatments, their interactions, and/or a plant's population of origin significantly differed in N-use efficiency ($N = 238$), P-use efficiency ($N = 238$), P_{NUE} ($N = 117$), and P_{PUE} ($N = 65$).

Foliar terpene concentrations

Separate ANOVA models were used to examine whether total, mono-, di-, and/or sesquiterpenes ($N = 58$; all log-transformed) significantly differed among cytotypes, soil-N:P treatments, their interaction, and/or a plant's population of origin.

RESULTS

Genome size variation among cytotypes

Holoploid and monoploid GS significantly differed among cytotypes but not between populations of the same cytotype (Appendix S2). Specifically, hexaploids had the largest, tetraploids intermediate, and diploids the smallest holoploid GS (2C-DNA content LS means ± 1 SE: $2x = 1.99 \pm 0.01$ pg, $4x = 3.55 \pm 0.02$ pg, $6x = 5.43 \pm 0.02$ pg). Diploids had the largest, hexaploids intermediate, and tetraploids the smallest monoploid GS (1Cx-DNA content LS means ± 1 SE: $2x = 0.99 \pm 0.003$ pg, $4x = 0.89 \pm 0.005$ pg, $6x = 0.90 \pm 0.004$ pg).

Material costs and biomass differences among cytotypes

Cellular but not tissue N and P material investments significantly differed among cytotypes (Appendix S3) with hexaploids having the highest, tetraploids intermediate, and diploids the least [N] and [P] per cell (Figure 1). Furthermore, soil-nutrient treatments together significantly affected N but not P investments, with plants having the highest [N] per cell and per tissue when grown under enriched-N and ambient-P conditions and the lowest [N] per cell and per tissue when grown under both ambient-N and ambient-P conditions (Appendix S3). While population of origin significantly affected [N] and [P] per cell and per milligram tissue, no other factors nor interaction among factors significantly affected investment patterns (Appendix S3).

Cytotype and N treatment both had a significant effect on aboveground biomass although the effects of N treatment depended separately upon cytotype and P treatment (Appendix S4). In general, aboveground biomass was greater for plants in enriched-N treatments and increased with ploidy level (Figure 2; Appendix S4). However, under enriched-N treatments tetraploids and hexaploids did not significantly differ from each other but had greater aboveground biomasses than diploids (controlled contrast: $F_{2,217} = 5.83$, $P = 0.0034$; Figure 2A), whereas under ambient-N treatments, tetraploids and diploids did not significantly differ from each other and had lower aboveground biomasses than hexaploids did (controlled contrast: $F_{2,217} = 4.91$, $P = 0.0082$; Figure 2A). Cytotype and N treatment also both had a significant effect on belowground biomass although the effects of N treatment jointly depended upon cytotype and P treatment (Appendix S4). In particular, belowground biomasses were greater under enriched-N conditions and increased with ploidy level, but under ambient-P conditions, differences among cytotypes were more pronounced (controlled contrast: $F_{2,217} = 20.19$, $P < 0.0001$; Figure 2B) than under enriched-P conditions (controlled contrast: $F_{2,217} = 6.32$, $P = 0.0022$; Figure 2C). Furthermore, under enriched-P, belowground biomass of hexaploids did not vary under different N treatments (Figure 2C). Lastly, population of origin but no other factors significantly affected above- and belowground biomasses (Appendix S4).

Cumulatively, differences in above- and belowground biomass in response to factor variables were reflected in growth response patterns to nutrient amendments. Specifically, we found that the growth of cytotypes differed significantly in response to N but not to P amendments (Table 1); tetraploids had greater increases in growth after N-enrichment than did diploids and hexaploids, which did not significantly differ in growth (Figure 3).

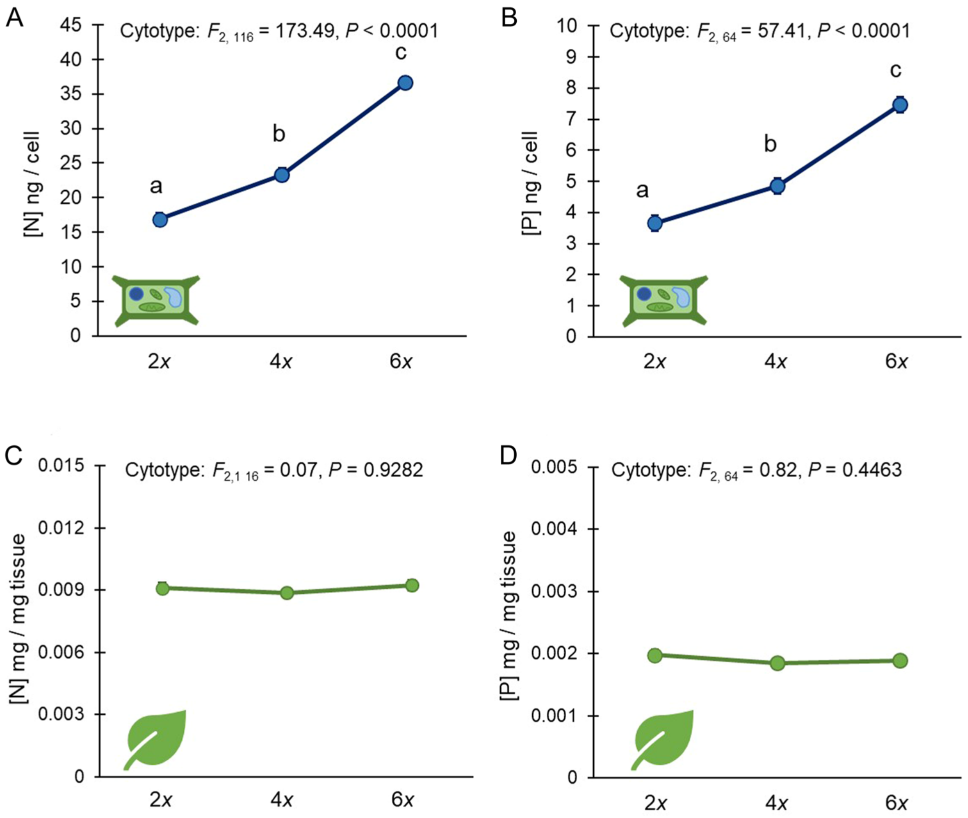

FIGURE 1 LS mean values ± 1 SE (error bars) for (A, B) [N] and [P] (ng/cell) and (C, D) for diploids (2*x*), tetraploids (4*x*), and hexaploids (6*x*) (mg/mg tissue). F_{df} and *P*-values for "cytotype" are given, and results of Tukey's HSD tests for significant differences between cytotypes are reported with different letters; see full statistical details in Appendix S3.

Transcriptome sizes

Transcriptome size and relative transcriptome size both significantly differed among cytotypes but not in the same way (Appendix S5). Specifically, hexaploids had the largest, tetraploids intermediate (although not significantly different from the other two cytotypes), and diploids had the smallest transcriptomes (Figure 4A), whereas diploids had significantly larger relative transcriptomes than tetraploids, which had slightly larger but not significantly different relative transcriptomes than hexaploids (Figure 4B). Plants also differed in transcriptome sizes dependent on treatments with plants in the ambient-N:P treatments yielding significantly more total RNA per cell than plants in the enriched-N:P treatments (LS means ± 1 SE: ambient-N:P = 32.36 ± 1.69 pg/cell, enriched-N:P = 27.56 ± 1.79 pg/cell; Appendix S5). No other factors nor interactions among factors significantly affected transcriptome attributes.

Photosynthesis, evapotranspiration, and water-use efficiency

Population of origin, cytotype, and N treatments all had a significant effect on A_{max} and E values, but the significance and direction of effects of cytotype and N-treatments depended upon P treatments (Table 2). To better discern response patterns, we used controlled contrasts to look at cytotype and N treatment differences separately under ambient- and enriched-P treatments, as P treatments alone did not significantly affect these attributes (Table 2). When values were averaged across nutrient treatments, diploids had greater A_{max} and E values than polyploids did (Figure 5), and when values were averaged across cytotypes, plants grown under enriched-N versus ambient-N conditions had greater A_{max} and E values (Figure 5). However, in the ambient P-treatments, differences in A_{max} and E were primarily driven by much greater responses of polyploids (especially tetraploids) than diploids to N addition (controlled contrasts for A_{max} in 2*x*: $F_{1,211} = 0.11$, $P = 0.7435$, 4*x*: $F_{1,211} = 19.82$, $P < 0.0001$, 6*x*: $F_{1,211} = 3.20$, $P = 0.0751$; for E in 2*x*: $F_{1,211} = 0.11$, $P = 0.7382$, 4*x*: $F_{1,211} = 20.34$, $P < 0.0001$, 6*x*: $F_{1,211} = 2.42$, $P = 0.1211$; Figure 5A, C), whereas under enriched-P treatments these patterns were primarily driven by much greater responses of diploids (especially for A_{max}) than polyploids to N-addition (controlled contrasts for A_{max} in 2*x*: $F_{1,211} = 4.73$, $P = 0.0307$, 4*x*: $F_{1,211} = 0.23$, $P = 0.6226$, 6*x*: $F_{1,211} = 0.00$, $P = 0.9877$; for E in 2*x*: $F_{1,211} = 2.98$, $P = 0.0858$, 4*x*: $F_{1,211} = 0.00$, $P = 0.9616$, 6*x*: $F_{1,211} = 0.01$, $P = 0.9264$; Figure 5B, D).

Water-use efficiencies significantly differed among N treatments, but significance independently varied among cytotypes and P treatments (Table 2). Specifically,

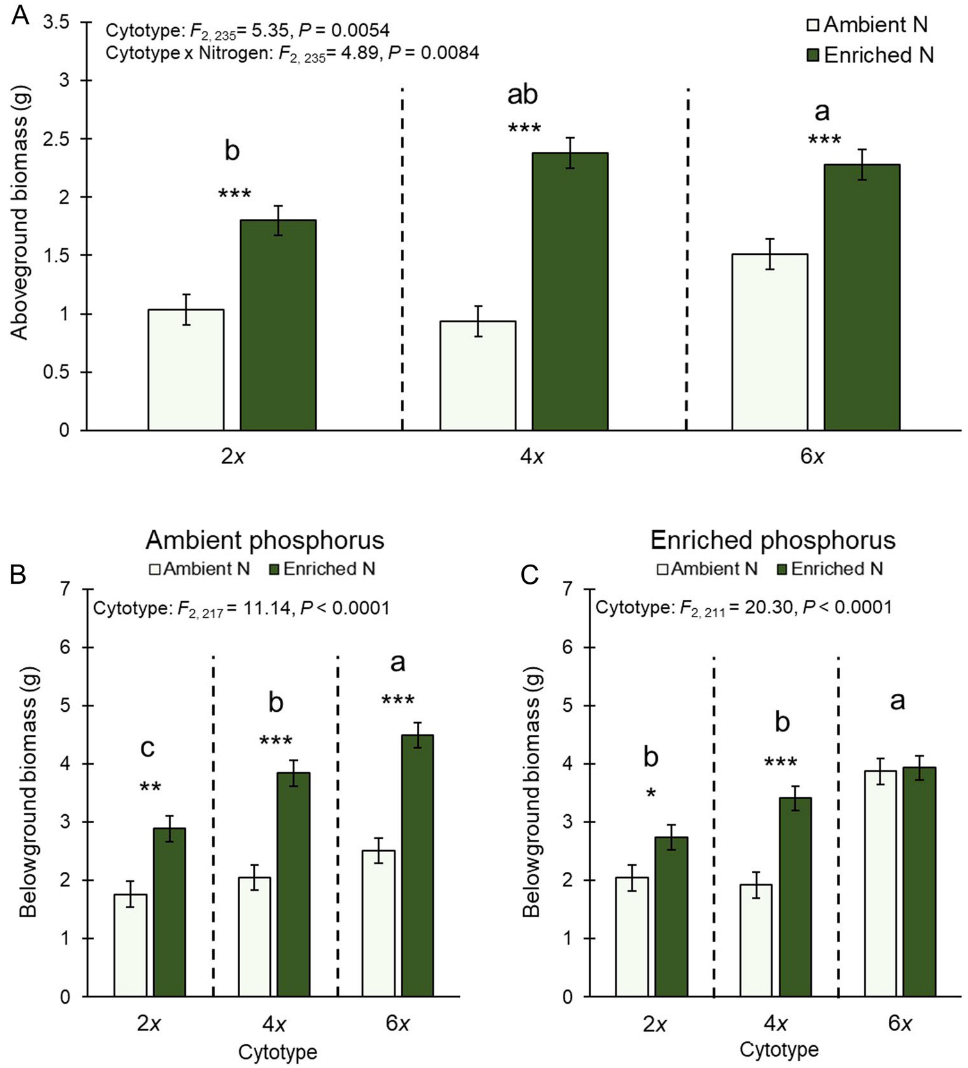

FIGURE 2 LS mean values ± SE (error bars) for (A) aboveground and (B, C) belowground biomass for the significant interactions of plant cytotype ($2x$ = diploid, $4x$ = tetraploid, $6x$ = hexaploid) and (A) N availability alone and (B, C) under ambient or enriched phosphorus availabilities. F_{df} and P-values are given for controlled contrasts testing for significant differences between cytotypes regardless of N treatment, which are reported with different letters. Controlled contrasts were also used to test for significant differences between ambient and enriched treatments within a single cytotype (reported in text); significant differences are noted with asterisks (*P < 0.05, **P < 0.001, ***P < 0.0001). Full statistical details are in Appendix S4.

polyploids had significantly higher WUE_i values than diploids did and their WUE_i values were highest when grown in ambient-N treatments, whereas diploid WUE_i values did not vary dependent upon N-treatments (controlled contrasts for WUE_i between ambient-N and enriched-N treatments for $2x$: $F_{1,211} = 0.11$, $P = 0.7389$, $4x$: $F_{1,211} = 11.03$, $P = 0.0011$, $6x$: $F_{1,211} = 4.94$, $P = 0.0273$, Figure 6). Furthermore, plants grown in ambient-N and in P treatments generally had higher WUE_i values than in all the other treatments (LS means ± 1 SE: ambient-N:ambient-P = 0.77 ± 0.03 μmol CO_2 mmol H_2O^{-1}, enriched-N:ambient-P = 0.64 ± 0.03 μmol CO_2 mmol H_2O^{-1}, ambient-N:enriched-P = 0.68 ± 0.03 μmol CO_2 mmol H_2O^{-1}, enriched-N:enriched-P = 0.66 ± 0.03 μmol CO_2 mmol H_2O^{-1}; Table 2). Lastly, population of origin had a significant effect on both A_{max} and E, but no other factors significantly affected A_{max}, E, and WUE_i (Table 2).

Nutrient-use efficiencies

Nitrogen-use efficiencies (NUEs) differed among plants grown in the different N treatments contingent upon cytotype or P treatments (Table 3). Specifically, plants were more efficient at incorporating N into biomass when grown under ambient-N and enriched-P treatments (Table 3; Figure 7A), but under ambient-N treatments, hexaploids used N significantly more efficiently than the other cytotypes did regardless of P treatment (controlled contrasts between cytotypes in enriched-N: $F_{2,217} = 2.82$, $P = 0.0615$; in ambient-N: $F_{2,217} = 13.10$, $P < 0.0001$; Figure 7B). Furthermore, P-use efficiencies (PUEs) significantly differed among plants grown in ambient-N and enriched-N treatments, but such differences were dependent upon P treatment and cytotype (Table 3). In general, plants more efficiently incorporated P into biomass when grown under both ambient-P and enriched-N (Table 3; Figure 7C), but regardless of the P treatment, hexaploids incorporated P into biomass significantly more efficiently than diploids and tetraploids under ambient-N but not under enriched-N treatments (controlled contrasts between cytotypes in enriched-N: $F_{2,217} = 4.79$, $P = 0.0092$; in ambient-N: $F_{2,217} = 3.06$, $P = 0.0489$; Figure 7D).

Differences in photosynthetic nutrient-use efficiencies were dependent upon 3-way interactions between cytotype, N treatment, and P treatment (Table 3). Because P treatments alone did not significantly affect photosynthetic nutrient-use efficiencies, we used controlled contrasts to look at cytotype and N-treatment differences separately under ambient-P and enriched P-treatments. Under ambient-P treatments, cytotypes differed in their ability to use N and P to fix CO_2, but significance and patterns depended upon N treatment (Table 3; Appendix S6). Specifically, tetraploids, but not the other cytotypes, required more N and P to fix CO_2 (lower P_{NUE} and P_{PUE} values) when grown in ambient-N versus enriched-N treatments (controlled contrasts under enriched-N versus ambient-N treatments for P_{NUE} for 2*x*: $F_{1,97} = 3.12$, $P = 0.0803$, 4*x*: $F_{1,97} = 8.10$, $P = 0.0054$, 6*x*: $F_{1,97} = 1.20$, $P = 0.2756$; for P_{PUE} for 2*x*: $F_{1,46} = 0.45$, $P = 0.5075$, 4*x*: $F_{1,46} = 11.72$, $P = 0.0013$, 6*x*: $F_{1,46} = 0.65$, $P = 0.4245$; Table 3; Appendix S6). Under enriched-P treatments, cytotypes and populations significantly differed in P_{NUE}, but not in P_{PUE}; diploids were more efficient at using N to fix CO_2 than tetraploids and hexaploids (controlled contrast between cytotypes in enriched-P treatments for P_{NUE}: $F_{2,97} = 4.63$, $P = 0.0118$; LS means ± 1 SE in μmol CO_2 m^{-2} s^{-1}/mg N per mg tissue for $2x = 152.57 \pm 9.71$, $4x = 112.37 \pm 11.23$, $6x = 117.74 \pm 10.24$). Lastly, population of origin had a significant effect on NUE and PUE, but no other factors nor interaction among factors significantly affected NUE, PUE, P_{NUE}, or P_{PUE} values (Table 3).

TABLE 1 Results from fixed-effects ANOVA models for the effects of cytotype (diploid = 2*x*, tetraploid = 4*x*, hexaploid = 6*x*) on above- and belowground growth responses to N and P. Bold values indicate a significant effect at $\alpha = 0.05$, and if a factor was found to be significant, we determined significant differences between means with Tukey's HSD tests ($\alpha = 0.05$; as reported here).

Source[a]	df	MS	*F*	Prob > *F*	Tukey's HSD[b]
Aboveground growth response to N					
Cytotype	2	1.00	4.82	**0.0165**	4*x* (=2*x*) > 6*x* (=2*x*)
Model error	20	0.20			
Aboveground growth response to P					
Cytotype	2	0.13	0.52	0.6031	
Model error	20	0.25			
Belowground growth response to N					
Cytotype	2	0.49	4.38	**0.0230**	4*x* (=2*x*) > 6*x* (=2*x*)
Model error	20	0.11			
Belowground growth response to P					
Cytotype	2	0.02	0.20	0.8176	
Model Error	20	0.10			

[a]Overall model significance for aboveground growth response to N: $R^2 = 0.27$, $F_{2,28} = 4.82$, $P = 0.0165$, $N = 29$; aboveground growth response to P: $R^2 = 0.04$, $F_{2,28} = 0.52$, $P = 0.6031$, $N = 29$; belowground growth response to N: $R^2 = 0.25$, $F_{2,28} = 4.38$, $P = 0.0230$, $N = 29$; belowground growth response to P: $R^2 = 0.02$, $F_{2,28} = 0.20$, $P = 0.8176$, $N = 29$.

[b]Cytotype LS means ± 1 SE: aboveground growth response to N: $2x = 0.40 \pm 0.14$, $4x = 0.84 \pm 0.14$, $6x = 0.23 \pm 0.15$; belowground growth response to N: $2x = 0.29 \pm 0.11$, $4x = 0.58 \pm 0.11$, $6x = 0.13 \pm 0.11$.

Foliar terpene concentrations

Foliar concentrations of terpenes significantly differed between cytotypes with diploids having higher concentrations of total,

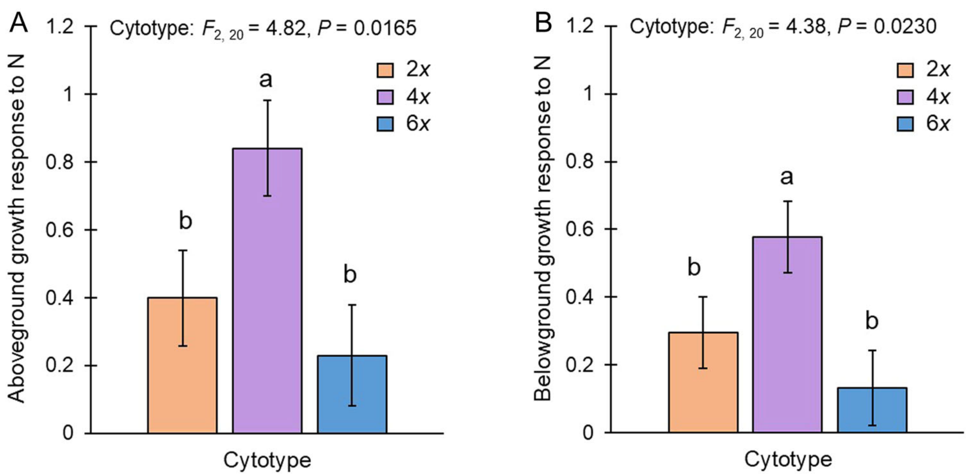

FIGURE 3 LS mean values ± 1 SE (error bars) for (A) aboveground and (B) belowground responses to N additions for diploids (2*x*), tetraploids (4*x*), and hexaploids (6*x*). F_{df} and *P*-values for cytotype are given and results of Tukey's HSD tests for significant differences between cytotypes are reported with different letters; full statistical details are in Table 1.

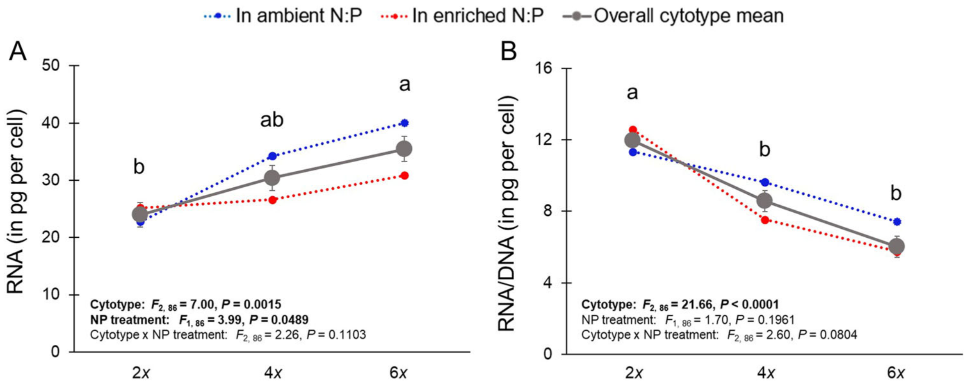

FIGURE 4 LS mean values ± 1 SE (error bars) for (A) total RNA concentration ([RNA]) per cell (pg/cell) and (B) relative transcriptome size ([RNA]/[2C-DNA content]) showing the significant effects of (A, B) ploidy and (A) soil N:P treatment. F_{df} and *P*-values for cytotype, N and P treatment, and their interaction is given and the results of Tukey's HSD tests for significant differences between cytotypes are reported with different letters. Full statistical details are in Appendix S5.

monoterpenes, and sesquiterpenes than tetraploids and hexaploids, which did not differ from each other and diploids and tetraploids having similar but greater concentrations of diterpenes than hexaploids (LS means ± 1 SE in Table 4, Appendix S7). Surprisingly, plants grown under ambient-N:P conditions had significantly higher foliar total terpene and monoterpene concentrations than plants grown under enriched-N:P conditions (LS means ± 1 SE in Table 4). No other model factors nor interactions among factors significantly affected foliar terpene concentrations (Table 4).

DISCUSSION

The adaptive potential of WGD in the absence of hybridization in angiosperms has been debated (Comai, 2005; Mayrose et al., 2015; Van de Peer et al., 2017; Doyle and Coate, 2019). In comparison to diploid progenitors, several studies using autopolyploid species report that polyploids are more abundant and have larger ranges in certain environments and/or regions (Schlaepfer et al., 2008; Kim et al., 2012; Krejčíková et al., 2013; Liu et al., 2019), but this pattern is not universal (Semple, 1984; Molgo et al., 2017). Such patterns may reflect polyploid versus diploid advantage that is nutrient dependent because organisms with larger genomes, such as polyploids, are more constrained by nutrient limitations but benefit more, in terms of productivity and biological functioning, from nutrient enrichments (Šmarda et al., 2013; Guignard et al., 2016; Bales and Hersch-Green, 2019; Peng et al., 2022). Here, we explored whether cytotype advantages in the *Solidago gigantea* complex depend upon nutrients. Specifically, we tested the hypotheses that NP material costs increase with ploidy level and thus lead to trade-offs between cell synthesis, metabolic activity, and trait expression that favor diploids in nutrient-limiting conditions, but upon release of nutrient constraints favor polyploids. We grew diploid and autopolyploid *S. gigantea* plants under ambient and enriched NP soil conditions and found evidence that N and P cellular costs, but not tissue material costs, increase with ploidy level, but that some traits and resource strategies might minimize these greater material-cost constraints and/or influence ecological dynamics and patterns of selection. We discuss our findings in terms of how nutrient-dependent cytotype advantages might influence ecoevolutionary dynamics and cytogeographic patterns specifically within *S. gigantea* and more broadly within flowering plants.

Material costs are greater in polyploids

We found several lines of evidence indicating that material costs increase with GS in *S. gigantea*. First, cellular [N] and [P] increased from diploids to tetraploids to hexaploids, which suggests increased elemental costs from synthesizing longer DNA strands (Sterner and Elser, 2002; Elser et al., 2011) and phospholipid membranes associated with enlarged cells (Leitch and Bennett, 2004; Cavalier-Smith, 2005; Roddy et al., 2020). Second, as others have shown (Coate and Doyle, 2010; Schoenfelder and Fox, 2015; Doyle and Coate, 2019; Song et al., 2020; Yahya et al., 2022), we found that total RNA content per cell increased with ploidy level and because RNA is also composed of strings of nucleic acids with a sugar–phosphate backbone, such increases in RNA content would also increase NP cellular costs. Third, because plants that are more limited by resources tend to experience greater growth benefits when these resources are added (Boyer, 1982), we also expected to find stronger positive relationships between growth responses to nutrient enrichments in plants with a higher ploidy level (Lewis, 1985; Leitch and Bennett, 2004; Cavalier-Smith, 2005; Faizullah et al., 2021). Here, while all cytotypes had positive growth responses to nutrient enrichments (indicating nutrient limitations to growth), tetraploids were the most responsive to N enrichment, a

TABLE 2 Results from fixed-effects ANOVA models for the effects of cytotype (diploid = 2*x*, tetraploids = 4*x*, hexaploid = 6*x*), soil N treatment (ambient = A, enriched = E), soil P treatment (A, E), their interactions, and population nested within cytotype on maximum photosynthetic rate (A_{max}), evapotranspiration rate (E), and instantaneous water-use efficiency (WUE_i). Bold values indicate a significant effect at $\alpha = 0.05$. If model factors were found to be significant, we determined significant differences between means with Tukey's HSD tests ($\alpha = 0.05$; as reported here) or with controlled contrasts as detailed and reported in the main text.

Source[a]	df	MS	*F*	Prob > *F*	Tukey's HSD[b,c,d,e]
A_{max}					
Cytotype (C)	2	233.16	19.86	**<0.0001**	2*x* > 4*x* = 6*x*
Nitrogen (N)	1	183.13	15.60	**0.0001**	E > A
Phosphorus (P)	1	5.63	0.48	0.4895	
C × N	2	14.22	1.21	0.2999	
C × P	2	4.96	0.42	0.6559	
N × P	1	36.08	3.07	0.0811	
C × N × P	2	53.14	4.53	**0.0119**	See Results
Population [C]	8	55.25	4.71	**<0.0001**	
Model error	211	11.74			
E					
Cytotype (C)	2	27.74	32.93	**<0.0001**	2*x* > 4*x* = 6*x*
Nitrogen (N)	1	9.31	11.05	**0.0010**	E > A
Phosphorus (P)	1	0.65	0.77	0.3812	
C × N	2	1.14	1.36	0.2592	
C × P	2	0.79	0.94	0.3932	
N × P	1	3.10	3.68	0.0563	
C × N × P	2	3.65	4.33	**0.0143**	See Results
Population [C]	8	2.99	3.55	**0.0012**	
Model error	211	0.84			
WUE_i					
Cytotype (C)	2	1.38	33.49	**<0.0001**	6*x* = 4*x* > 2*x*
Nitrogen (N)	1	0.37	8.92	**0.0032**	A > E
Phosphorus (P)	1	0.08	1.95	0.1640	
C × N	2	0.14	3.45	**0.0335**	See Results
C × P	2	0.00	0.11	0.8965	
N × P	1	0.18	4.25	**0.0404**	AA (=AE) > EE = EA (=AE)
C × N × P	2	0.09	2.07	0.1286	
Population [C]	8	0.08	1.94	0.0652	
Model error	211	0.04			

[a]Overall significance model for A_{max}: $R^2 = 0.36$, $F_{18,230} = 6.59$, $P < 0.0001$, $N = 230$; E: $R^2 = 0.42$, $F_{18,230} = 8.55$, $P > 0.0001$, N = 230; WUE_i: $R^2 = 0.41$, $F_{18,230} = 8.11$, $P < 0.0001$, $N = 230$.

[b]Cytotype LS means ± 1 SE for A_{max}: 2*x* = 10.59 ± 0.41, 4*x* = 8.29 ± 0.78, 6*x* = 8.28 ± 0.52 μmol CO_2 m^{-2} s^{-1}; *E*: 2*x* = 2.31 ± 0.11, 4*x* = 1.17 ± 0.11, 6*x* = 1.26 ± 0.14 mmol H_2O m^{-2} s^{-1}; WUE_i: 2*x* = 0.52 ± 0.02, 4*x* = 0.76 ± 0.02, 6*x* = 0.78 ± 0.03 μmol CO_2 mmol H_2O^{-1}.

[c]Nitrogen LS means ± 1 SE for A_{max}: ambient N = 8.19 ± 0.40, enriched N = 9.92 ± 0.42 μmol CO_2 m^{-2} s^{-1}; *E*: ambient N = 1.38 ± 0.09, enriched N = 1.78 ± 0.09 mmol H_2O m^{-2} s^{-1}; WUE_i: ambient N = 0.73 ± 0.02, enriched N = 0.65 ± 0.02 μmol CO_2 mmol H_2O^{-1}.

[d]Cytotype × N LS means ± 1 SE for WUE_i are reported in Figure 6.

[e]N × P LS means ± 1 SE for WUE_i: ambient-N:ambient-P = 0.77 ± 0.03, ambient-N:enriched-P = 0.68 ± 0.03, enriched-N:ambient-P = 0.64 ± 0.03, enriched-N:enriched-P = 0.66 ± 0.03 μmol CO_2 mmol H_2O^{-1}.

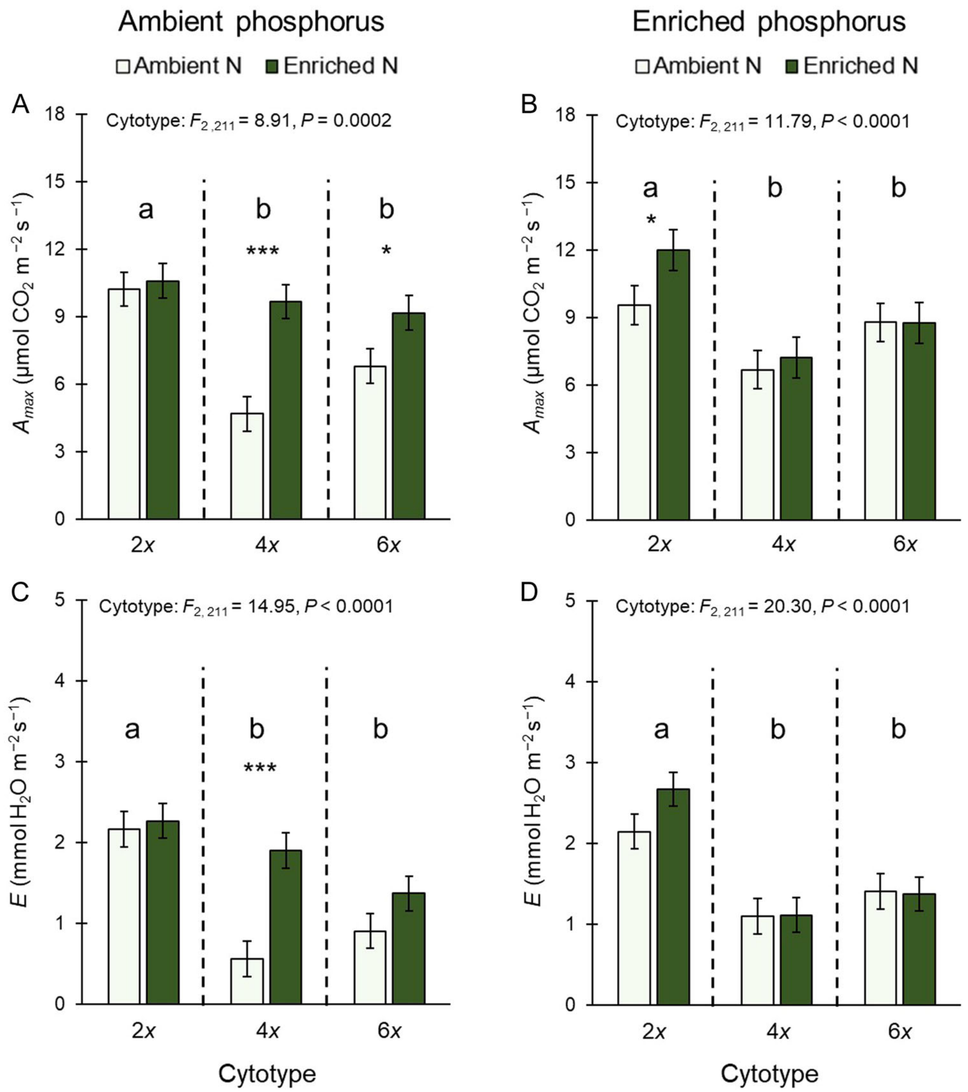

FIGURE 5 LS mean values ± 1 SE (error bars) for (A, B) maximum photosynthetic rate (A_{max}), and (C, D) evapotranspiration rate (E) showing the significant effects of the interaction between cytotype and nitrogen availability under ambient and enriched phosphorus availabilities. F_{df} and P-values are given for controlled contrasts testing for significant differences between cytotypes regardless of N treatment and indicated by different letters. Controlled contrasts were also used to test for significant differences between ambient and enriched treatments within a single cytotype (reported in text), and significant differences are noted with asterisks (*$P < 0.05$, **$P < 0.001$, ***$P < 0.0001$). Full statistical details are in Table 2.

finding that indirectly suggests that tetraploids are more limited by N than diploids or hexaploids are.

Interestingly, and in contrast to our predictions, hexaploids, despite having higher cellular material costs, were not the most responsive in terms of growth to N enrichment and had a growth response comparable to that of diploids. Several factors might contribute to this response. First, the greater ability of hexaploids to more efficiently turn nutrients into biomass in ambient-N conditions may have contributed to their more muted growth responses to N-enrichment because they were able to produce large aboveground biomasses in both ambient-N and enriched-N treatments. This ability could be due to the fact that, relative to tetraploids, growth in hexaploids is accomplished more by cell expansion than by cell division (as found in other larger-celled polyploids, Greilhuber and Leitch, 2013), which would be less costly in terms of NP investment to growth. Second, differences in monoploid GS (1Cx-DNA content; total amount of DNA in unreplicated chromosome sets; Greilhuber et al., 2005) may have also contributed to the muted growth responses of hexaploids to N enrichment. For example, while both holoploid ([2C-DNA content]; total amount of DNA in replicated chromosome sets) and monoploid GSs have been found to be positively correlated with size-related traits and negatively correlated with cell division and growth-related rates (Wyngaard et al., 2005; Beaulieu et al., 2008), holoploid GS has been more strongly correlated with the former and monoploid GS with the latter (Rhind and Gilbert, 2013; Suda et al., 2015). Thus, while organisms with larger

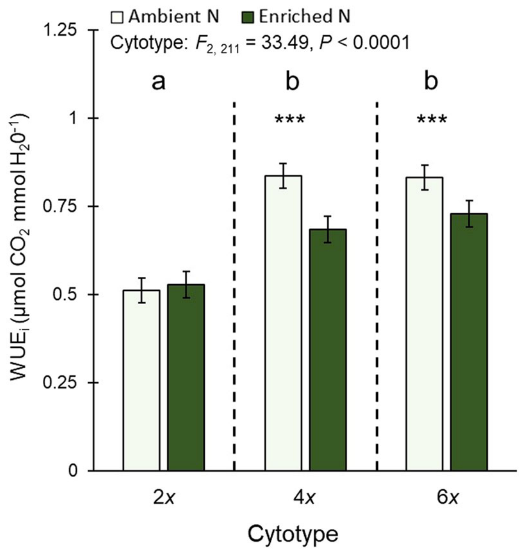

FIGURE 6 LS mean values ± 1 SE (error bars) for instantaneous water-use efficiency (WUE_i) for the significant interactions between cytotype and nitrogen availability. F_{df} and P-values are given for controlled contrasts testing for significant differences between cytotypes regardless of N treatment, which are indicated with different letters. Controlled contrasts were also used to test for significant differences between ambient and enriched treatments within a single cytotype (reported in text). Significant differences are noted with asterisks ($*P < 0.05$, $**P < 0.001$, $***P < 0.0001$). Full statistical details are in Table 2.

genomes typically grow slower (Wyngaard et al., 2005; Beaulieu et al., 2008), downsizing of the monoploid-genome might counteract the extra time typically needed to replicate and organize extra chromosome copies during cell division. Therefore, a downsized monoploid genome should be correlated with faster cell division rates and responsiveness to nutrients for both tetraploids and hexaploids, but hexaploids, with larger holoploid GS, might be further constrained by increased material costs. In addition, faster cell division rates associated with smaller monoploid GS might have been offset by the additional time needed to replicate, check, and repair the six replicates of each hexaploid chromosome during the S and G2 phases of cell division. Third, several studies have found that polyploids have increased associations with microbes (Wu et al., 2019; Forrester et al., 2020) and/or arbuscular mycorrhizal fungi (Anneberg and Segraves, 2019) relative to closely related diploids and that such differences might ameliorate nutrient acquisitions and contribute to the differential growth responses of the cytotypes to nutrients. Although we did not examine whether rhizospheric differences among cytotypes influenced the nutrient-exchange networks of *S. gigantea*, a post hoc analysis of N uptake efficiency (a measure of N in plant biomass relative to N in soil) showed that under ambient-N inputs, hexaploids were the most efficient at incorporating N into plant biomass (Appendix S8). Lastly, differences in growth and physiological responses among cytotypes to nutrients may partially be obscured by population differences in adaptative processes whereby different populations have had different lengths of time to adapt (presumably shorter in polyploids) and/or are locally adapted to different environmental conditions. While we cannot assess this possibility and contribution using field-collected maternal lines, we did find that population of origin had a significant effect on growth, metabolic, and nutrient-use attributes. Thus, hexaploids in general might not have been as negatively affected as tetraploids (or even diploids) in terms of biomass accumulation under ambient-N conditions if hexaploids are pre-adapted to tolerate the more N-poor conditions of the Great Plains versus the less nitrogen-poor conditions of the Great Lakes and eastern regions (Smith et al., 2022) where tetraploids and diploids primarily occur, respectively.

Genetic mechanisms might minimize material-cost constraints

Greater material costs should theoretically translate into reduced plant growth and competitive success and stronger selective constraints, but various genetic mechanisms that act over long- and short-evolutionary time periods may minimize the higher GS material costs of polyploids. For example, over long evolutionary periods, genome downsizing could reduce material costs (Wang et al., 2021a), and we found consistent evidence for genome downsizing in *S. gigantea* (i.e., polyploids had smaller monoploid GS than diploids did), which did not significantly vary among populations of the same cytotype. While some studies have reported more extreme genome downsizing in higher ploidy levels (Leitch and Bennett, 2004; Wang et al., 2021a), we found less evidence for genome downsizing in hexaploids than in tetraploids, which could arise either because there was less time for genome elimination in hexaploids since they likely arose after tetraploids, and/or because some duplicated segments of the genome are needed for stability and/or are adaptive (Leitch and Bennett, 2004; Zenil-Ferguson et al., 2016; Wang et al., 2021a) so there may be a lower limit to genome downsizing.

Over short evolutionary time periods, reductions in transcriptome sizes could also minimize realized material costs and selective constraints. For example, the transcriptome is a large cellular N and P sink (Raven, 2013), but transcriptome material costs vary depending upon the identity and number of transcripts expressed at any given time. Therefore, organisms may limit their total material costs by reducing overall gene expression (Faizullah et al., 2021; Wang et al., 2021a), and several studies have reported that organisms that experience resource limitations have smaller transcriptomes (Wu et al., 2004; Forieri et al., 2017; Kelly, 2018; Majda et al., 2021). We found that despite polyploids producing on average more total RNA per cell, they had smaller relative transcriptome sizes (RNA/DNA) than diploids, suggesting that transcriptome downsizing could help alleviate material-cost constraints in the

TABLE 3 Results from fixed-effects ANOVA models for the effects of cytotype (diploid = 2*x*, tetraploids = 4*x*, hexaploid = 6*x*), soil N treatment (ambient = A, enriched = E), soil P treatment (A, E), their interactions, and population nested within cytotype on N-use efficiency (NUE), P-use efficiency (PUE), photosynthetic N-use efficiency (P_{NUE}), and photosynthetic P-use efficiency (P_{PUE}). Bold values indicate a significant effect at $\alpha = 0.05$. If model factors were found to be significant, we determined significant differences between means with Tukey's HSD tests ($\alpha = 0.05$; as reported here) or with controlled contrasts as detailed and reported in the main text.

Source[a]	df	MS	*F*	Prob > *F*	Tukey's HSD[b,c,d,e]
NUE					
Cytotype (C)	2	2.89×10^{-3}	7.36	**0.0008**	6*x* > 4*x* = 2*x*
Nitrogen (N)	1	9.20×10^{-4}	2.34	0.1279	
Phosphorus (P)	1	1.42×10^{-3}	3.61	0.0588	
C × N	2	3.27×10^{-3}	8.29	**0.0003**	See Results
C × P	2	1.10×10^{-3}	2.78	0.0640	
N × P	1	5.84×10^{-3}	14.82	**0.0002**	AE (=EA) > EE = AA (=EA)
C × N × P	2	1.02×10^{-3}	2.59	0.0771	
Population [C]	7	1.53×10^{-3}	3.05	**0.0005**	
Model error	217	3.94×10^{-4}			
PUE					
Cytotype (C)	2	0.0438	1.82	**0.0146**	6*x* (=4*x*) > 2*x* (=4*x*)
Nitrogen (N)	1	1.0427	34.77	**<0.0001**	E > A
Phosphorus (P)	1	0.9774	26.68	**<0.0001**	A > E
C × N	2	0.0318	4.02	**0.0460**	See 'Results'
C × P	2	0.0057	1.24	0.5743	
N × P	1	0.3818	5.79	**<0.0001**	EA > EE = AA > AE
C × N × P	2	0.0024	1.17	0.7865	
Population [C]	7	0.0404	2.09	**0.0004**	
Model error	217	0.0102			
P_{NUE}					
Cytotype (C)	2	20156.47	12.35	**<0.0001**	2*x* > 4*x* = 6*x*
Nitrogen (N)	1	7295.00	4.47	**0.0371**	E > A
Phosphorus (P)	1	4716.51	2.89	0.0924	
C × N	2	1077.95	0.66	0.5190	
C × P	2	253.60	0.16	0.8563	
N × P	1	250.43	0.15	0.6962	
C × N × P	2	9541.38	5.84	**0.0040**	See Results
Population [C]	7	4720.76	2.89	**0.0087**	
Model error	97	1632.66			
P_{PUE}					
Cytotype (C)	2	135.15	1.48	0.2376	
Nitrogen (N)	1	291.50	3.20	0.0803	
Phosphorus (P)	1	33.34	0.37	0.5482	
C × N	2	86.18	0.95	0.3958	
C × P	2	42.90	0.47	0.6275	

TABLE 3 (Continued)

Source[a]	df	MS	*F*	Prob > *F*	Tukey's HSD[b,c,d,e]
N × P	1	49.11	0.54	0.4666	
C × N × P	2	346.31	3.80	**0.0297**	See Results
Population [C]	7	143.04	1.57	0.1685	
Model error	46	91.13			

[a]Overall significance model for NUE: $R^2 = 0.34$, $F_{18,235} = 6.12$, $P < 0.0001$; PUE: $R^2 = 0.57$, $F_{18,235} = 16.11$, $P < 0.000$; P_{NUE}: $R^2 = 0.44$, $F_{18,115} = 4.22$, $P < 0.0001$, $N = 116$; P_{PUE}: $R^2 = 0.42$, $F_{18,64} = 1.87$, $P = 0.0453$, $N = 65$.

[b]Cytotype LS means ± 1 SE: N-use efficiency (g plant tissue/mg N soil): 2*x* = 0.04 ± 0.002, 4*x* = 0.04 ± 0.002, 6*x* = 0.05 ± 0.003; PUE (g plant tissue/mg P in soil): 2*x* = 0.17 ± 0.012, 4*x* = 0.20 ± 0.012, 6*x* = 0.23 ± 0.003; P_{NUE} (μmol CO_2 m^{-2} s^{-1}/mg N/mg tissue^{-1}): 2*x* = 143.27 ± 6.82, 4*x* = 96.70 ± 6.58, 6*x* = 112.07 ± 8.26.

[c]Nitrogen LS means ± 1 SE: PUE (g plant tissue/mg P in soil): ambient N = 0.13 ± 0.009; enriched N = 0.26 ± 0.009; P_{NUE} (μmol CO_2 m^{-2} s^{-1} per mg N per mg tissue $^{-1}$): ambient N = 109.38 ± 5.60; enriched N = 125.32 ± 5.67.

[d]Phosphorus LS means ± 1 SE: PUE (g plant tissue/mg P in soil): ambient P = 0.26 ± 0.009; enriched P = 0.13 ± 0.009.

[e]LS means for factor interactions: see Appendix S6.

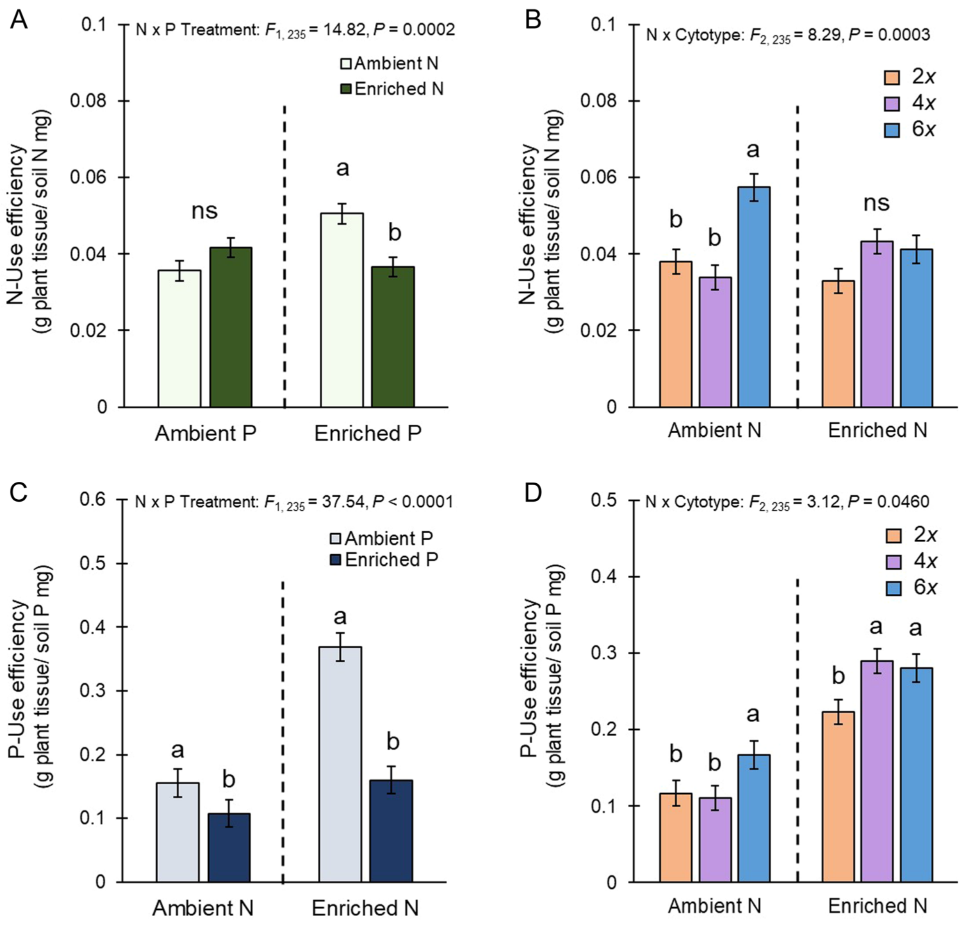

FIGURE 7 LS Mean values ± 1 SE (error bars) for (A, B) N-use efficiency and (C, D) P-use efficiency for the significant interactions (A, C) between nitrogen and phosphorus availability and (B, D) between plant cytotype (2*x* = diploid, 4*x* = tetraploid, 6*x* = hexaploid) and nitrogen availability. F_{df} and *P*-values for interactions (A, C) between nitrogen (N) × phosphorus (P) and (B, D) N × cytotypes are given in the figure, and significant differences between means were determined with controlled contrasts (reported in text). Significant differences between (A) N treatments, (C) P treatments, and (B, D) cytotypes are noted with different letters; full statistical details are in Table 3.

short term. However, contrary to our expectations, differences in total and relative transcriptome sizes among polyploids and diploids were not more pronounced under nutrient-limiting conditions, suggesting that transcriptome downsizing may help minimize material cost increases with GS independently of nutrient context and/or local adaptive processes. As a caveat, observed differences in total RNA production per cell may not be entirely predictive of

TABLE 4 Results from fixed-effects ANOVA models for the effects of cytotype (diploid = $2x$, tetraploids = $4x$, hexaploid = $6x$), soil N:P treatments (ambient N:P = A, enriched N:P = E), their interaction, and population of origin nested within cytotype on the concentrations of foliar total terpenes, monoterpenes, diterpenes, and sesquiterpenes (all log-transformed). Bold values indicate a significant effect at α = 0.05, and Tukey's HSD test (α = 0.05) were used to determine significant differences between cytotype and treatment means (as reported here).

Source[a]	df	MS	*F*	Prob > *F*	Tukey's HSD[b,c]
Total terpenes					
Cytotype (C)	2	13.41	9.57	**0.0003**	$2x > 4x = 6x$
Treatment (T)	1	3.95	5.65	**0.0213**	A > E
C × T	2	0.54	0.38	0.6830	
Population [C]	7	2.76	3.94	**0.0017**	
Model error	50	0.70			
Total monoterpenes					
Cytotype (C)	2	12.70	7.12	**0.0012**	$2x > 4x = 6x$
Treatment (T)	1	3.92	4.75	**0.0340**	E > A
C × T	2	0.38	0.46	0.6353	
Population [C]	7	3.07	3.73	**0.0025**	
Model error	50	0.82			
Total diterpenes					
Cytotype (C)	2	6.24	4.43	**0.0169**	$4x = 2x > 6x$
Treatment (T)	1	0.15	0.11	0.7442	
C × T	2	0.30	0.21	0.8095	
Population [C]	7	1.38	0.98	0.4571	
Model error	50	1.41			
Total sesquiterpenes					
Cytotype (C)	2	5.80	4.88	**0.0116**	$2x > 4x = 6x$
Treatment (T)	1	3.14	2.64	0.1103	
C × T	2	0.19	0.16	0.8539	
Population [C]	7	1.43	1.20	0.3206	
Model error	50	1.19			

[a]Overall model significance for total terpenes: $R^2 = 0.58$, $F_{12,62} = 5.77$, $P < 0.0001$, $N = 63$; total monoterpenes: $R^2 = 0.55$, $F_{12,62} = 5.05$, $P < 0.0001$, $N = 63$; total diterpenes: $R^2 = 0.29$, $F_{12,62} = 1.66$, $P = 0.1047$, $N = 63$, (insignificant overall ANOVA model negates any factor significance); total sesquiterpenes: $R^2 = 0.38$, $F_{12,62} = 2.54$, $P = 0.0106$, $N = 63$.

[b]Cytotype LS nontransformed means ± 1 SE for total terpenes: $2x = 7.43 \pm 0.77$, $4x = 3.35 \pm 0.76$, $6x = 1.56 \pm 1.31$ mg/mg tissue; for monoterpenes: $2x = 6.89 \pm 0.73$, $4x = 3.09 \pm 0.71$; $6x = 1.45 \pm 1.23$ mg/mg tissue; for diterpenes: $2x = 0.06 \pm 0.01$, $4x = 0.06 \pm 0.01$, $6x = 0.02 \pm 0.02$ mg/mg tissue; for sesquiterpenes: $2x = 0.48 \pm 1.46$, $4x = 0.20 \pm 0.14$,$6x = 0.09 \pm 0.25$ mg/mg tissue.

[c]Nutrient treatment LS nontransformed means ± 1 SE for total terpenes: ambient NP = 5.12 ± 0.76, enriched NP = 3.10 ± 0.71 mg/mg tissue; for monoterpenes: ambient NP = 4.89 ± 0.71, enriched NP = 2.73 ± 0.67; mg/mg tissue.

material costs because different RNA sequences, whether coding or noncoding, require different amounts of N and P atoms for synthesis (Elser et al., 2011; Raven, 2013) such that there is not a 1:1 relationship between RNA production and NP material costs. Furthermore, we measured total RNA production from one time period in a single leaf, but transcriptome regulation, and therefore material costs, can vary over ontogeny (Takacs et al., 2012; Shinozaki et al., 2018; Leiboff and Hake, 2019) and different parts of organisms (Matas et al., 2011; Zhang et al., 2020; Sun et al., 2021), and thus total transcriptome material costs may not be reflected by a single leaf measurement. Lastly, while we used the same protocol to extract RNA from all samples and checked for repeatability, RNA extractions might vary according to cell size, which could affect our findings. While we cannot rule out this methodological explanation, we believe that it is unlikely because we found that transcriptome downsizing was greater than genome downsizing, with tetraploids producing about 66% of the total diploid leaf RNA (putative parents), a number which closely mirrors results found in other polyploid plant systems using different methods of RNA extraction and transcriptome quantification (Coate and Doyle, 2010; Doyle and Coate, 2019).

Resource investment trade-offs and acquisition strategies might minimize material-cost constraints but alter ecological interactions and patterns of selection

N and P atoms are also used in primary and secondary metabolic processes, such as photosynthesis (Evans, 1989; Hessen et al., 2010; Hohmann-Marriott and Blankenship, 2011) and as precursors to defensive compound synthesis (Bohlmann et al., 1998; Bustamante et al., 2020). Therefore, on the basis of increased material costs, we predicted that polyploids would be more constrained by nutrient availabilities and would invest less into these costly processes under ambient nutrient conditions (Kelly, 2018; Faizullah et al., 2021), but that as nutrients increased, they would invest proportionately more into these processes. We found partial support for this hypothesis in that diploids tended to have the highest photosynthetic rates and typically produced the highest amounts of terpenes. However, despite the observation that polyploids tended to have more reduced photosynthetic activity relative to diploids when both N and P were at ambient levels, differences among cytotypes in terpene production and photosynthetic rates were not less apparent under enriched nutrient conditions. Furthermore, in contrast to our predictions, larger GS cytotypes were not more efficient than smaller GS cytotypes at incorporating N and P into photosynthates or biomass (although under ambient conditions, hexaploids were the most efficient at incorporating nutrients into biomass, which might be related to them being more adapted to nutrient-poor soils; Smith et al., 2022). Cumulatively, these results suggest that larger GS cytotypes might use resources more efficiently (as seen in hexaploids) and/or partition resources between the genome and other costly factions (such as photosynthesis and defense) to lessen genome-material-cost constraints but that the extent of these processes may vary dependent upon unique population-specific, selective processes.

Differences in metabolic processes and resource allocation might further influence ecological interactions, which could indirectly affect how genome-material costs alter patterns of selection. For instance, despite having larger genomes from WGD events, and thus putatively more genes for defense compounds (i.e., gene dosage effects, neo- and/or sub-functionalization; Comai, 2005), polyploids produced lower amounts of defense compounds than diploids, even under enriched-NP conditions, which may make them more susceptible to consumptive antagonists. Reduced photosynthetic activity might also be ecologically costly to polyploids if it contributes to reduced growth and competitive ability. However, despite diploids having higher photosynthetic and evapotranspiration rates than polyploids, polyploids had significantly higher WUEs than in diploids, suggesting that increases in GS had less of a negative effect on photosynthetic rates than on evapotranspiration rates in our experiment. Studies involving other species have also found that higher stomata density was associated with greater reductions in stomatal conductance and evapotranspiration rates than photosynthetic rates (Lawson and Blatt, 2014). Furthermore, polyploid but not diploid WUE_i values were significantly higher under ambient-N than enriched-N conditions, and elevated WUE may selectively favor polyploids when nutrients and water are both limiting. The balance between conserving material costs and ecological costs versus benefits in polyploids is likely complex and dependent upon multiple interacting abiotic (e.g., water availability, soil composition) and biotic (e.g., symbiotic associations, antagonist pressures) factors.

CONCLUSIONS

We found that N and P cellular material costs increased with ploidy level in *S. gigantea* but that various mechanisms and trade-offs might lessen material costs and alter ecological constraints on polyploids. Our findings potentially provide insight into the observed cytogeographic patterning and lack of mixed-ploidy populations found in *S. gigantea*, as variations in available soil nutrients and/or water availability at both large and small scales could contribute to the differential colonization and ecological success of some cytotypes over others. More generally, as N and P availabilities are increasing (Penuelas et al., 2013; Fowler et al., 2015; Goyette et al., 2016; Asabere et al., 2018) and precipitation patterns are changing across ecosystems worldwide, nutrient enrichments could result in a large-scale release from GS-mediated nutrient constraints in many plant species, especially large GS polyploids, which ultimately could affect individual fitness and competitive performances of plant species dependent upon their GS or ploidy level (Šmarda et al., 2013; Guignard et al., 2016; Peng et al., 2022). Although we found consistent and significant differences among cytotypes, we also found that different populations of the same cytotype might respond differently in terms of growth, physiology, and resource-use to variation in environmental attributes. In polyploid complexes, such as *S. gigantea*, where cytotypes are widely spatially and ecologically segregated and rarely co-occur, local environmental conditions and time of population origin (presumably later for polyploids than diploids), could also influence adaptive processes affecting material-cost constraints and trade-offs. Additional studies should explore relationships between GS variation and resource allocation/investment trade-offs within polyploid complexes with co-occurring cytotypes (to minimize uncertainties in patterns due to local adaptation to different environments) and more broadly across the angiosperm phylogeny to enhance our mechanistic understanding of whether and how increased material costs due to increases in GS alter species and community ecoevolutionary dynamics. Such studies would be incredibly beneficial in strengthening the predictive frameworks related to how multispecies communities might respond to globally changing environments.

AUTHOR CONTRIBUTIONS

The experiment was designed by E.H.-G. with input from and set-up by A.W. E.H.-G. and A.W. collected, analyzed, and interpreted data and wrote the manuscript.

ACKNOWLEDGMENTS

We thank Alexis Shatrau and Brianna Wieferich for data collection assistance. This work was funded by an NSF CAREER grant awarded to E.H.-G. (Award # 1941309), the Department of Biological Sciences, and the Ecosystem Science Center at Michigan Technological University, Houghton, MI. We thank Simeon Schum for GC-MS analysis of terpene extracts and assisting in data interpretation and Carsten Külheim for RNA extraction assistance. We also thank *AJB* Associate Editor R. Brandon Pratt and two anonymous reviewers whose comments improved this manuscript.

CONFLICTS OF INTEREST STATEMENT

The authors report no conflicts of interest.

DATA AVAILABILITY STATEMENT

Data files used in statistical analyses will be available from the Dryad Digital Repository: https://doi.org/10.5061/dryad.931zcrjrm (Walczyk and Hersch-Green, 2023).

ORCID

Angela M. Walczyk http://orcid.org/0000-0003-3656-7861
Erika I. Hersch-Green http://orcid.org/0000-0003-3887-0768

REFERENCES

Acquisti, C., J. J. Elser, and S. Kumar. 2009a. Ecological nitrogen limitation shapes the DNA composition of plant genomes. *Molecular Biology and Evolution* 26: 953–956.

Acquisti, C., S. Kumar, and J. J. Elser. 2009b. Signatures of nitrogen limitation in the elemental composition of the proteins involved in the metabolic apparatus. *Proceedings of the Royal Society, B, Biological Sciences* 276: 2605–2610.

Anneberg, T. J., and K. A. Segraves. 2019. Intraspecific polyploidy correlates with colonization by arbuscular mycorrhizal fungi in *Heuchera cylindrica*. *American Journal of Botany* 106: 894–900.

Anneberg, T. J., and K. A. Segraves. 2020. Nutrient enrichment and neopolyploidy interact to increase lifetime fitness of *Arabidopsis thaliana*. *Plant and Soil* 456: 439–453.

Asabere, S. B., T. Zeppenfeld, K. A. Nketia, and D. Sauer. 2018. Urbanization leads to increases in pH, carbonate, and soil organic matter stocks of arable soils of Kumasi, Ghana (West Africa). *Frontiers in Environmental Science* 6: 119.

Bales, A. L., and E. I. Hersch-Green. 2019. Effects of soil nitrogen on diploid advantage in fireweed, *Chamerion angustifolium* (Onagraceae). *Ecology and Evolution* 9: 1095–1109.

Barker, M. S., N. Arrigo, A. E. Baniaga, Z. Li, and D. A. Levin. 2016. On the relative abundance of autopolyploids and allopolyploids. *New Phytologist* 210: 391–398.

Beaulieu, J. M., I. J. Leitch, S. Patel, A. Pendharkar, and C. A. Knight. 2008. Genome size is a strong predictor of cell size and stomatal density in angiosperms. *New Phytologist* 179: 975–986.

Birchler, J. A., and R. A. Veitia. 2010. The gene balance hypothesis: implications for gene regulation, quantitative traits and evolution. *New Phytologist* 186: 54–62.

Blommaert, J. 2020. Genome size evolution: towards new model systems for old questions. *Proceedings of the Royal Society, B, Biological Sciences* 287: 20201441.

Bohlmann, J., G. Meyer-Gauen, and R. Croteau. 1998. Plant terpenoid synthases: molecular biology and phylogenetic analysis. *Proceedings of the National Academy of Sciences, USA* 95: 4126–4133.

Boyer, J. S. 1982. Plant productivity and environment. *Science* 218: 443–448.

Bragg, J. G., and A. Wagner. 2009. Protein material costs: Single atoms can make an evolutionary difference. *Trends in Genetics* 25: 5–8.

Brown, R., and P. Rickless. 1949. A new method for the study of cell division and cell extension with some preliminary observations on the effect of temperature and of nutrients. *Proceedings of the Royal Society of London, B, Biological Sciences* 136: 110–125.

Bustamante, M. Á., M. Michelozzi, A. Barra Caracciolo, P. Grenni, J. Verbokkem, P. Geerdink, C. Safi, and I. Nogues. 2020. Effects of soil fertilization on terpenoids and other carbon-based secondary metabolites in *Rosmarinus officinalis* plants: a comparative study. *Plants* 9: 830.

Cao, Q., X. Zhang, X. Gao, L. Wang, and G. Jia. 2018. Effects of ploidy level on the cellular, photochemical and photosynthetic characteristics in *Lilium* FO hybrids. *Plant Physiology and Biochemistry* 133: 50–56.

Cavalier-Smith, T. 2005. Economy, speed and size matter: evolutionary forces driving nuclear genome miniaturization and expansion. *Annals of Botany* 95: 147–175.

Chen, Y., H. Xu, T. He, R. Gao, G. Guo, R. Lu, Z. Chen, and C. Liu. 2021. Comparative analysis of morphology, photosynthetic physiology, and transcriptome between diploid and tetraploid barley derived from microspore culture. *Frontiers in Plant Science* 12: 283.

Chen, Z. J. 2007. Genetic and epigenetic mechanisms for gene expression and phenotypic variation in plant polyploids. *Annual Review of Plant Biology* 58: 377–406.

Choi, H.-K., J.-H. Mun, D.-J. Kim, H. Zhu, J.-M. Baek, J. Mudge, B. Roe, N. Ellis, J. Doyle, G. B. Kiss, N. D. Young, and D. R. Cook. 2004. Estimating genome conservation between crop and model legume species. *Proceedings of the National Academy of Sciences, USA* 101: 15289–15294.

Christou, M., E. J. Avramides, J. P. Roberts, and D. L. Jones. 2005. Dissolved organic nitrogen in contrasting agricultural ecosystems. *Soil Biology and Biochemistry* 37: 1560–1563.

Coate, J. E., and J. J. Doyle. 2010. Quantifying whole transcriptome size, a prerequisite for understanding transcriptome evolution across species: an example from a plant allopolyploid. *Genome Biology and Evolution* 2: 534–546.

Comai, L. 2005. The advantages and disadvantages of being polyploid. *Nature Reviews Genetics* 6: 836–846.

Corneillie, S., N. De Storme, R. Van Acker, J. U. Fangel, M. De Bruyne, R. De Rycke, D. Geelen, et al. 2018. Polyploidy affects plant growth and alters cell wall composition *Plant Physiology* 179: 74–87.

Dobjanschi, L., L. Fritea, E. B. Patay, and M. Tamas. 2019. Comparative study of the morphological and phytochemical characterization of Romanian *Solidago* species. *Pakistan Journal of Pharmaceutical Sciences* 32: 1571–1579.

Dodsworth, S., A. R. Leitch, and I. J. Leitch. 2015. Genome size diversity in angiosperms and its influence on gene space. *Current Opinion in Genetics & Development* 35: 73–78.

Doyle, J. J., and J. E. Coate. 2019. Polyploidy, the nucleotype, and novelty: the impact of genome doubling on the biology of the cell. *International Journal of Plant Sciences* 180: 1–52.

Elser, J. J., C. Acquisti, and S. Kumar. 2011. Stoichiogenomics: the evolutionary ecology of macromolecular elemental composition. *Trends in Ecology & Evolution* 26: 38–44.

Enke, N., J. Fuchs, and B. Gemeinholzer. 2011. Shrinking genomes? Evidence from genome size variation in *Crepis* (Compositae). *Plant Biology* 13: 185–193.

Evans, J. R. 1989. Photosynthesis and nitrogen relationships in leaves of C_3 plants. *Oecologia* 78: 9–19.

Faizullah, L., J. A. Morton, E. I. Hersch-Green, A. M. Walczyk, A. R. Leitch, and I. J. Leitch. 2021. Exploring environmental selection on genome size in angiosperms. *Trends in Plant Science* 26: 1039–1049.

Forieri, I., C. Sticht, M. Reichelt, N. Gretz, M. J. Hawkesford, M. Malagoli, M. Wirtz, and R. Hell. 2017. System analysis of metabolism and the transcriptome in *Arabidopsis thaliana* roots reveals differential co-regulation upon iron, sulfur and potassium deficiency. *Plant, Cell & Environment* 40: 95–107.

Forrester, N. J., M. Rebolleda-Gómez, J. L. Sachs, and T.-L. Ashman. 2020. Polyploid plants obtain greater fitness benefits from a nutrient acquisition mutualism. *New Phytologist* 227: 944–954.

Fowler, D., C. E. Steadman, D. Stevenson, M. Coyle, R. M. Rees, U. Skiba, M. Sutton, et al. 2015. Effects of global change during the 21st century on the nitrogen cycle. *Atmospheric Chemistry and Physics* 15: 13849–13893.

Gaynor, M. L., S. Lim-Hing, and C. M. Mason. 2020. Impact of genome duplication on secondary metabolite composition in non-cultivated species: a systematic meta-analysis. *Annals of Botany* 126: 363–376.

Goyette, J. O., E. M. Bennett, R. W. Howarth, and R. Maranger. 2016. Changes in anthropogenic nitrogen and phosphorus inputs to the St. Lawrence sub-basin over 110 years and impacts on riverine export. *Global Biogeochemical Cycles* 30: 1000–1014.

Graça, J., G. Bondi, A. Schmalenberger, and K. Daly. 2022. Phosphorus fractions in temperate grassland soils and their interactions with agronomic P tests. *Agronomy* 12: 2569.

Greilhuber, J., J. Doležel, M. A. Lysák, and M. D. Bennett. 2005. The origin, evolution and proposed stabilization of the terms 'genome size' and 'C-value' to describe nuclear DNA contents. *Annals of Botany* 95: 255–260.

Greilhuber, J., and I. J. Leitch. 2013. Genome size and the phenotype. *In* J. Greilhuber, J. Dolezel, and J. Wendel. [eds.], Plant genome diversity, 2. Springer, Vienna, Austria.

Grover, C., J. Gallagher, E. Szadkowski, M. Yoo, L. Flagel, and J. Wendel. 2012. Homoeolog expression bias and expression level dominance in allopolyploids. *New Phytologist* 196: 966–971.

Guignard, M. S., R. A. Nichols, R. J. Knell, A. Macdonald, C. A. Romila, M. Trimmer, I. J. Leitch, and A. R. Leitch. 2016. Genome size and ploidy influence angiosperm species' biomass under nitrogen and phosphorus limitation. *New Phytologist* 210: 1195–1206.

Hessen, D. O., M. Daufresne, and H. P. Leinaas. 2013. Temperature–size relations from the cellular–genomic perspective. *Biological Reviews* 88: 476–489.

Hessen, D. O., P. D. Jeyasingh, M. Neiman, and L. J. Weider. 2010. Genome streamlining and the elemental costs of growth. *Trends in Ecology & Evolution* 25: 75–80.

Hikosaka, K. 2004. Interspecific difference in the photosynthesis–nitrogen relationship: patterns, physiological causes, and ecological importance. *Journal of Plant Research* 117: 481–494.

Hloušková, P., T. Mandáková, M. Pouch, P. Trávníček, and M. A. Lysak. 2019. The large genome size variation in the *Hesperis* clade was shaped by the prevalent proliferation of DNA repeats and rarer genome downsizing. *Annals of Botany* 124: 103–120.

Hohmann-Marriott, M. F., and R. E. Blankenship. 2011. Evolution of photosynthesis. *Annual Review of Plant Biology* 62: 515–548.

Hull-Sanders, H. M., R. H. Johnson, H. A. Owen, and G. A. Meyer. 2009. Effects of polyploidy on secondary chemistry, physiology, and performance of native and invasive genotypes of *Solidago gigantea* (Asteraceae). *American Journal of Botany* 96: 762–770.

Islam, S., J. Zhang, Y. Zhao, M. She, and W. Ma. 2021. Genetic regulation of the traits contributing to wheat nitrogen use efficiency. *Plant Science* 303: 110759.

Jeyasingh, P. D., and L. J. Weider. 2007. Fundamental links between genes and elements: evolutionary implications of ecological stoichiometry. *Molecular Ecology* 16: 4649–4661.

Jiao, Y., N. J. Wickett, S. Ayyampalayam, A. S. Chanderbali, L. Landherr, P. E. Ralph, L. P. Tomsho, et al. 2011. Ancestral polyploidy in seed plants and angiosperms. *Nature* 473: 97–100.

Johnson, R. H., H. M. Hull-Sanders, and G. A. Meyer. 2007. Comparison of foliar terpenes between native and invasive *Solidago gigantea*. *Biochemical Systematics and Ecology* 35: 821–830.

Kang, M., J. Wang, and H. Huang. 2015. Nitrogen limitation as a driver of genome size evolution in a group of *Karst* plants. *Scientific Reports* 5: 11636.

Kelly, S. 2018. The amount of nitrogen used for photosynthesis modulates molecular evolution in plants. *Molecular Biology and Evolution* 35: 1616–1625.

Kim, S., A. L. Rayburn, A. Parrish, and D. K. Lee. 2012. Cytogeographic distribution and genome size variation in prairie cordgrass (*Spartina pectinata* Bosc ex Link). *Plant Molecular Biology Reporter* 30: 1073–1079.

Knight, C. A., and J. M. Beaulieu. 2008. Genome size scaling through phenotype space. *Annals of Botany* 101: 759–766.

Krejčíková, J., R. Sudová, K. C. Oberlander, L. L. Dreyer, and J. Suda. 2013. Cytogeography of *Oxalis pes-caprae* in its native range: Where are the pentaploids? *Biological Invasions* 15: 1189–1194.

Lawson, T., and M. R. Blatt. 2014. Stomatal size, speed, and responsiveness impact on photosynthesis and water use efficiency. *Plant Physiology* 164: 1556–1570.

Leiboff, S., and S. Hake. 2019. Reconstructing the transcriptional ontogeny of maize and sorghum supports an inverse hourglass model of inflorescence development. *Current Biology* 29: 3410–3419.e3413.

Leitch, I., and M. Bennett. 2004. Genome downsizing in polyploid plants. *Biological Journal of the Linnean Society* 82: 651–663.

Levin, D. A. 2019. Plant speciation in the age of climate change. *Annals of Botany* 124: 769–775.

Lewis, W. M. 1985. Nutrient scarcity as an evolutionary cause of haploidy. *American Naturalist* 125: 692–701.

Liu, K., W. Meng, L. Zheng, L. Wang, and S. Zhou. 2019. Cytogeography and chromosomal variation of the endemic east asian herb *Lycoris radiata*. *Ecology & Evolution* 9: 6849–6859.

Majda, S., D. Beisser, and J. Boenigk. 2021. Nutrient-driven genome evolution revealed by comparative genomics of chrysomonad flagellates. *Communications Biology* 4: 1–11.

Masson, P., T. Dalix, and S. Bussiere. 2010. Determination of major and trace elements in plant samples by inductively coupled plasma–mass spectrometry. *Communications in Soil Science and Plant Analysis* 41: 231–243.

Matas, A. J., T. H. Yeats, G. J. Buda, Y. Zheng, S. Chatterjee, T. Tohge, L. Ponnala, et al. 2011. Tissue- and cell-type specific transcriptome profiling of expanding tomato fruit provides insights into metabolic and regulatory specialization and cuticle formation. *Plant Cell* 23: 3893–3910.

Mayrose, I., S. H. Zhan, C. J. Rothfels, N. Arrigo, M. S. Barker, L. H. Rieseberg, and S. P. Otto. 2015. Methods for studying polyploid diversification and the dead end hypothesis: a reply to Soltis et al. (2014). *New Phytologist* 206: 27–35.

Molgo, I. E., D. E. Soltis, and P. S. Soltis. 2017. Cytogeography of *Callisia* section *cuthbertia* (Commelinaceae). *Comparative Cytogenetics* 11: 553–577.

Moll, R., E. Kamprath, and W. Jackson. 1982. Analysis and interpretation of factors which contribute to efficiency of nitrogen utilization 1. *Agronomy Journal* 74: 562–564.

Mueller, R. L. 2015. Genome biology and the evolution of cell-size diversity. *Cold Spring Harbor Perspectives in Biology* 7: a019125.

Neiman, M., A. Kay, and A. Krist. 2013. Can resource costs of polyploidy provide an advantage to sex? *Heredity* 110: 152–159.

Ninkuu, V., L. Zhang, J. Yan, Z. Fu, T. Yang, and H. Zeng. 2021. Biochemistry of terpenes and recent advances in plant protection. *International Journal of Molecular Science* 22: 5710.

Osborn, T. C., J. C. Pires, J. A. Birchler, D. L. Auger, Z. J. Chen, H.-S. Lee, L. Comai, et al. 2003. Understanding mechanisms of novel gene expression in polyploids. *Trends in Genetics* 19: 141–147.

Otto, S. P., and J. Whitton. 2000. Polyploid incidence and evolution. *Annual Review of Genetics* 34: 401–437.

Parisod, C., and O. Broennimann. 2016. Towards unified hypotheses of the impact of polyploidy on ecological niches. *New Phytologist* 212: 540–542.

Peng, Y., J. Yang, I. J. Leitch, M. S. Guignard, E. W. Seabloom, D. Cao, F. Zhao, et al. 2022. Plant genome size modulates grassland community responses to multi-nutrient additions. *New Phytologist* 236: 2091–2102.

Penuelas, J., B. Poulter, J. Sardans, P. Ciais, M. Van Der Velde, L. Bopp, O. Boucher, et al. 2013. Human-induced nitrogen–phosphorus imbalances alter natural and managed ecosystems across the globe. *Nature Communications* 4: 1–10.

Qiu, F., E. J. Baack, K. D. Whitney, D. G. Bock, H. M. Tetreault, L. H. Rieseberg, and M. C. Ungerer. 2019. Phylogenetic trends and environmental correlates of nuclear genome size variation in *Helianthus* sunflowers. *New Phytologist* 221: 1609–1618.

Ramsey, J., and D. W. Schemske. 2002. Neopolyploidy in flowering plants. *Annual Review of Ecology and Systematics* 33: 589–639.

Raven, J. A. 2013. RNA function and phosphorus use by photosynthetic organisms. *Frontiers in Plant Science* 4: 536.

Rhind, N., and D. M. Gilbert. 2013. DNA replication timing. *Cold Spring Harbor Perspectives in Biology* 5: a010132.

Robinson, D. E., R. G. Wagner, F. W. Bell, and C. J. Swanton. 2001. Photosynthesis, nitrogen-use efficiency, and water-use efficiency of jack pine seedlings in competition with four boreal forest plant species. *Canadian Journal of Forest Research* 31: 2014–2025.

Roddy, A. B., G. Théroux-Rancourt, T. Abbo, J. W. Benedetti, C. R. Brodersen, M. Castro, S. Castro, et al. 2020. The scaling of genome size and cell size limits maximum rates of photosynthesis with implications for ecological strategies. *International Journal of Plant Sciences* 181: 75–87.

Sánchez Vilas, J., and J. R. Pannell. 2017. No difference in plasticity between different ploidy levels in the mediterranean herb *Mercurialis annua*. *Scientific Reports* 7: 9484.

Schlaepfer, D. R., P. J. Edwards, J. C. Semple, and R. Billeter. 2008. Cytogeography of *Solidago gigantea* (Asteraceae) and its invasive ploidy level. *Journal of Biogeography* 35: 2119–2127.

Schoenfelder, K. P., and D. T. Fox. 2015. The expanding implications of polyploidy. *Journal of Cell Biology* 209: 485–491.

Semple, J. C. 1984. Cytogeographic studies on north american asters. I. Range surveys of *Virgulus adnatus*, *V. concolor*, *V. georgianus*, *V. grandiflorus*, *V. novae-angliae, V. oblongifolius*, *V. patens*, and *V. walteri*. *American Journal of Botany* 71: 522–531.

Shinozaki, Y., P. Nicolas, N. Fernandez-Pozo, Q. Ma, D. J. Evanich, Y. Shi, Y. Xu, et al. 2018. High-resolution spatiotemporal transcriptome mapping of tomato fruit development and ripening. *Nature Communications* 9: 364.

Simonin, K. A., and A. B. Roddy. 2018. Genome downsizing, physiological novelty, and the global dominance of flowering plants. *PLoS Biology* 16: e2003706.

Šmarda, P., M. Hejcman, A. Březinová, L. Horová, H. Steigerová, F. Zedek, P. Bureš, et al. 2013. Effect of phosphorus availability on the selection of species with different ploidy levels and genome sizes in a long-term grassland fertilization experiment. *New Phytologist* 200: 911–921.
Smith, E. M., R. Vargas, M. Guevara, T. Tarin, and R. V. Pouyat. 2022. Spatial variability and uncertainty of soil nitrogen across the conterminous united states at different depths. *Ecosphere* 13: e4170.
Soltis, P. S., and D. E. Soltis. 2000. The role of genetic and genomic attributes in the success of polyploids. *Proceedings of the National Academy of Sciences, USA* 97: 7051–7057.
Song, K., P. Lu, K. Tang, and T. C. Osborn. 1995. Rapid genome change in synthetic polyploids of Brassica and its implications for polyploid evolution. *Proceedings of the National Academy of Science, USAs* 92: 7719–7723.
Song, Q., A. Ando, N. Jiang, Y. Ikeda, and Z. J. Chen. 2020. Single-cell RNA-seq analysis reveals ploidy-dependent and cell-specific transcriptome changes in *Arabidopsis* female gametophytes. *Genome Biology* 21: 178.
Stebbins, G. L. 1950. Variation and evolution in plants. Columbia University Press, NY, NY, USA.
Stebbins, G. L. 1971. Chromosomal evolution in higher plants. Edward Arnold, London, UK.
Sterner, R. W., and J. J. Elser. 2002. Ecological stoichiometry: The biology of elements from molecules to the biosphere. Princeton University Press, Princeton, NJ, USA.
Suda, J., L. A. Meyerson, I. J. Leitch, and P. Pyšek. 2015. The hidden side of plant invasions: the role of genome size. *New Phytologist* 205: 994–1007.
Sun, T., J. Zhang, Q. Zhang, X. Li, M. Li, Y. Yang, J. Zhou, et al. 2021. Integrative physiological, transcriptome, and metabolome analysis reveals the effects of nitrogen sufficiency and deficiency conditions in apple leaves and roots. *Environmental and Experimental Botany* 192: 104633.
Takacs, E. M., J. Li, C. Du, L. Ponnala, D. Janick-Buckner, J. Yu, G. J. Muehlbauer, et al. 2012. Ontogeny of the maize shoot apical meristem. *Plant Cell* 24: 3219–3234.
Thébault, A., F. Gillet, H. Müller-Schärer, and A. Buttler. 2011. Polyploidy and invasion success: trait trade-offs in native and introduced cytotypes of two Asteraceae species. *Plant Ecology* 212: 315–325.
Théroux-Rancourt, G., A. B. Roddy, J. M. Earles, M. E. Gilbert, M. A. Zwieniecki, C. K. Boyce, D. Tholen, et al. 2021. Maximum CO2 diffusion inside leaves is limited by the scaling of cell size and genome size. *Proceedings of the Royal Society, B, Biological Sciences* 288: 20203145.
Van De Peer, Y., E. Mizrachi, and K. Marchal. 2017. The evolutionary significance of polyploidy. *Nature Reviews Genetics* 18: 411.
Verloove, F., B. J. Zonneveld, and J. C. Semple. 2017. First evidence for the presence of invasive *Solidago altissima* (Asteraceae) in Europe. *Willdenowia* 47: 69–75.
Veselý, P., P. Bureš, and P. Šmarda. 2013. Nutrient reserves may allow for genome size increase: Evidence from comparison of geophytes and their sister non-geophytic relatives. *Annals of Botany* 112: 1193–1200.
Vyas, P., M. S. Bisht, S.-I. Miyazawa, S. Yano, K. Noguchi, I. Terashima, and S. Funayama-Noguchi. 2007. Effects of polyploidy on photosynthetic properties and anatomy in leaves of *Phlox drummondii*. *Functional Plant Biology* 34: 673–682.
Wagner, A. 2007. From bit to it: How a complex metabolic network transforms information into living matter. *BMC Systems Biology* 1: 33.
Walczyk, A. and E. Hersch-Green. 2023. Data for: Genome material costs and functional tradeoffs in the autopolyploid *Solidago gigantea* (Giant Goldenrod) series. *Dryad, Dataset*. https://doi.org/10.5061/dryad.931zcrjrm
Walczyk, A. M. 2022. Investigating the role of genomic material costs in ecological, evolutionary, and invasion dynamics using the *Solidago gigantea* (giant goldenrod) polyploid complex. Ph.D. dissertation, Michigan Technological University, Digital Commons. Available at https://doi.org/10.37099/mtu.dc.etdr/1428
Walczyk, A. M., and E. I. Hersch-Green. 2019. Impacts of soil nitrogen and phosphorus levels on cytotype performance of the circumboreal herb *Chamerion angustifolium*: implications for polyploid establishment. *American Journal of Botany* 106: 906–921.
Walczyk, A. M., and E. I. Hersch-Green. 2022. Do water and soil nutrient scarcities differentially impact the performance of diploid and tetraploid *Solidago gigantea* (giant goldenrod, Asteraceae)? *Plant Biology* 24: 1031–1042.
Wang, X., J. A. Morton, J. Pellicer, I. J. Leitch, and A. R. Leitch. 2021a. Genome downsizing after polyploidy: mechanisms, rates and selection pressures. *Plant Journal* 107: 1003–1015.
Wang, Y., B. Jia, H. Ren, and Z. Feng. 2021b. Ploidy level enhances the photosynthetic capacity of a tetraploid variety of *Acer buergerianum* Miq. *PeerJ* 9: e12620.
Warner, D. A., and G. E. Edwards. 1993. Effects of polyploidy on photosynthesis. *Photosynthesis Research* 35: 135–147.
Wendel, J. F. 2015. The wondrous cycles of polyploidy in plants. *American Journal of Botany* 102: 1753–1756.
Wendel, J. F., S. A. Jackson, B. C. Meyers, and R. A. Wing. 2016. Evolution of plant genome architecture. *Genome Biology* 17: 1–14.
Wood, T. E., N. Takebayashi, M. S. Barker, I. Mayrose, P. B. Greenspoon, and L. H. Rieseberg. 2009. The frequency of polyploid speciation in vascular plants. *Proceedings of the National Academy of Sciences, USA* 106: 13875–13879.
Wu, J., N. Zhang, A. Hayes, K. Panoutsopoulou, and S. G. Oliver. 2004. Global analysis of nutrient control of gene expression in *Saccharomyces cerevisiae* during growth and starvation. *Proceedings of the National Academy of Sciences, USA* 101: 3148–3153.
Wu, S., J. Cheng, X. Xu, Y. Zhang, Y. Zhao, H. Li, and S. Qiang. 2019. Polyploidy in invasive *Solidago canadensis* increased plant nitrogen uptake, and abundance and activity of microbes and nematodes in soil. *Soil Biology and Biochemistry* 138: 107594.
Wyngaard, G. A., E. M. Rasch, N. M. Manning, K. Gasser, and R. Domangue. 2005. The relationship between genome size, development rate, and body size in copepods. *Hydrobiologia* 532: 123–137.
Yactayo-Chang, J. P., H. V. Tang, J. Mendoza, S. A. Christensen, and A. K. Block. 2020. Plant defense chemicals against insect pests. *Agronomy* 10: 1156.
Yahya, G., P. Menges, P. S. Amponsah, D. A. Ngandiri, D. Schulz, A. Wallek, N. Kulak, et al. 2022. Sublinear scaling of the cellular proteome with ploidy. *Nature Communications* 13: 6182.
Yang, X., J. Cheng, B. Yao, H. Lu, Y. Zhang, J. Xu, X. Song, et al. 2021. Polyploidy-promoted phenolic metabolism confers the increased competitive ability of *Solidago canadensis*. *Oikos* 130: 1014–1025.
Zenil-Ferguson, R., J. M. Ponciano, and J. G. Burleigh. 2016. Evaluating the role of genome downsizing and size thresholds from genome size distributions in angiosperms. *American Journal of Botany* 103: 1175–1186.
Zhang, J., Y. Wang, Y. Zhao, Y. Zhang, J. Zhang, H. Ma, and Y. Han. 2020. Transcriptome analysis reveals nitrogen deficiency induced alterations in leaf and root of three cultivars of potato (*Solanum tuberosum* L.). *PLoS One* 15: e0240662.

SUPPORTING INFORMATION

Additional supporting information can be found online in the Supporting Information section at the end of this article.

Appendix S1. Flow cytometry methods and population collection sites.

Appendix S2. Results from fixed-effect ANOVA models for the effects of cytotype and population nested within cytotype on holoploid and monoploid GS.

Appendix S3. Results from fixed-effects ANOVA models for the effects of cytotype, soil N treatment, soil P treatment, their interactions, and population nested within cytotype on [N] and [P] (ng/ng cell) and [N] and [P] (mg/mg leaf tissue).

Appendix S4. Results from fixed effects ANOVA models for the effects of cytotype, soil N treatment, soil P treatment, their interactions, and population nested within cytotype on above and belowground biomass (g).

Appendix S5. Results from fixed effects ANOVA models for the effects of cytotype, soil-N:P treatments, their interaction, and population nested within cytotype on transcriptome size ([RNA]) and relative transcriptome size ([RNA]/[2C-DNA content]) per cell.

Appendix S6. LS mean values ± SE for photosynthetic nitrogen-use efficiency and phosphorus-use efficiency for the significant interactions between plant cytotype and nitrogen treatment under ambient phosphorus conditions.

Appendix S7. Nontransformed LS mean values ± SE for total terpenes, monoterpenes, diterpenes, and sesquiterpenes for plant cytotypes.

Appendix S8. Results from fixed effects ANOVA models for the effects of cytotype, soil N treatment, soil P treatment, their interactions, and population nested within cytotype on N-uptake efficiency (mg N per g plant tissue per mg N in soil).

How to cite this article: Walczyk, A. M. and E. I. Hersch-Green. 2023. Genome-material costs and functional trade-offs in the autopolyploid *Solidago gigantea* (giant goldenrod) series. *American Journal of Botany* 110(9): e16218. https://doi.org/10.1002/ajb2.16218